Russian Chemical Reviews **70** (10) 809 – 825 (2001) © 2001 Russian Academy of Sciences and Turpion Ltd

DOI 10.1070/RC2001v070n10ABEH000671

Nanochemistry of metals

G B Sergeev

Contents

I.	Introduction	809
II.	Synthesis and chemical reactions of metal nanoparticles	809
III.	Cryonanochemistry of metals	813
IV.	Ensembles involving nanoparticles	815
V.	Photochemistry and nanophotonics	817
VI.	Semiconductors and sensors	818
VII.	Catalysis on nanoparticles	820
VIII.	Nanoparticles in biology and medicine	822
IX.	Conclusion	823

Abstract. The results of studies on the nanochemistry of metals published in recent years are generalised. Primary attention is centred on the methods for the synthesis of nanoparticles and their chemical reactions. The means of stabilisation of nanoparticles which involve individual metals and incorporate atoms of several metals are considered as well as their physicochemical properties. Self-assembling processes of nanoparticles are described. The prospects of using metal nanoparticles in semiconductor devices, catalysis, biology and medicine are discussed. The bibliography includes 165 references.

I. Introduction

The last decade of the XXth century was marked by the increased attention of scientists in the fields of physics, chemistry, materials science, *etc*. devoted to nanoparticles, *viz*., to their synthesis, properties and different reactions. The reason for this lies in the fact that particles of nanometer sizes exhibit peculiar mechanical, optical, electrical and magnetic properties different from those of the corresponding macroparticles. Since 1990, the annual growth in publications devoted to both nanoparticles themselves and the prospects of their application in nanotechnologies has been observed. The methods of synthesis and stabilisation of nanoparticles as well as their optical, magnetic and other properties have already been summarised. In particular, quite a number of books, collections of papers and surveys devoted to metal and semiconductor nanoparticles and materials fabricated on their basis have already been published.[1–15]

At the same time, studies on the chemical reactions that involve nanoparticles are still in their infancy, and even the keyword 'nanochemistry' has appeared in reference journals relatively recently. This review is intended to make up for this gap. It mainly deals with chemical reactions that involve metal nanoparticles; however, a special section is devoted to the synthesis, stabilisation and physicochemical properties of nanoparticles based on individual metals, several metals and metal compounds.

In this review, an attempt is undertaken to follow the main trends in the development of this new scientific field by considering studies published mostly in 2000. Primary attention is given to the use of low temperatures in studies on the activities of metal nanoparticles and size effects. (The question of how the particle size affects its reactivity still remains one of most challenging and stubborn questions of modern chemistry.[16]) Self-assembling of nanoparticles and their application in catalysis and photocatalysis are discussed. Major problems of the chemistry of nanoparticles and nanomaterials are considered and approaches to their solution are suggested.

II. Synthesis and chemical reactions of metal nanoparticles

Until recently, particles with sizes in the range from 1 to 100 nm were assigned to nanoparticles (in certain studies, this interval was even extended to 1000 nm), although, in accordance with the International System of Units (SI) (the prefix nano- is used for fraction units, *viz.,* 10^{-9}), nanoparticles should involve only particles with sizes in the range from 1 to 10 nm, and it is more correct to consider 100-nm particles as ultradispersed ones and the materials based on them as macroscopic materials.

Nanochemistry studies synthetic methods and chemical properties of particles with sizes of 1 – 10 nm. The most interesting problems of nanochemistry are concerned with the reactivity of nanoparticles. For example, chemical properties of 1-nm particles that contain $\sim$10 metal atoms can be changed by introduction of only one atom. This is why, it is important to know and correctly understand the chemical and physical regularities that govern the activities of particles with the sizes of an order of magnitude of 1 nm.

Investigation of the dependence of chemical and physical properties of nanoparticles on the number of constituent metal atoms and the nature of ligands bound to nanoparticles represents a new direction in nanochemistry. At present, this field accumulates the knowledge which will allow one to understand the effects of the geometry, electronic properties and sizes of such systems on their reactivities. Properties of nanoparticles synthesised in the gas

G B Sergeev Department of Chemistry, M V Lomonosov Moscow State University, Leninskie Gory, 119899 Moscow, Russian Federation.
Fax (7-095) 939 02 83. Tel. (7-095) 939 54 42.
E-mail: gbs@kinet.chem.msu.ru

Received 28 March 2001
Uspekhi Khimii **70** (10) 915 – 933 (2001); translated by T Ya Safonova

phase have been studied in more detail. The joint use of a supersonic jet, pulse lasers and mass spectrometry made it possible to obtain, identify and characterise 'free' nanoparticles containing different numbers of metal atoms. The dependence of the chemical activity of nanoparticles in the gas phase on the number of the constituent atoms was studied in detail for niobium [17] and iron [18] particles.

At present, attention is focused on the development of methods for the synthesis and stabilisation of nanoparticles in the liquid phase. Special attention is paid to the preparation of monodispersed particles.

1. Reduction in solution

Methods of chemical reduction play an important role in the solution of the problem of synthesis of monodispersed particles. These methods were mainly used for the synthesis of gold and silver nanoparticles and less often for platinum, cobalt, nickel and copper nanoparticles.

Spherical silver nanoparticles with sizes of 3.3–4.8 nm were synthesised by reduction of silver nitrate by sodium borohydride in the presence of bis[(trimethylammoniodecanoylamino)ethyl] disulfide dibromide as a stabiliser.[19] The particles obtained were characterised by active light absorption in the wavelength range near 400 nm, which corresponded to the silver plasmon peak and indicated the metallic nature of the particles. The environment effect on the stability of silver particles formed showed that the latter form aggregates in the presence of sulfuric and hydrochloric acids. The stability of silver particles was also shown to depend on the pH of the medium; at pH 5–9 in aqueous media, the particles remained stable for a week. Both an increase and a decrease in the pH resulted in fast aggregation and precipitation of silver particles. The effect of the pH on the stability of gold particles was less pronounced compared with silver particles.

Metal nanoparticles of controllable sizes (1–2 nm) were prepared using amphifillic poly(octadecylsiloxane) as a matrix.[20]

Hybrid matrices based on polyelectrolyte gels with oppositely charged surfactants were used as nanostructurised media for the reduction of various platinum salts by sodium borohydride and hydrazine. It was shown that with $NaBH_4$ as the reductant small platinum particles with radii of $\sim$2–3 nm were mainly formed, whereas the use of hydrazine resulted in particles of $\sim$40 nm.[21]

For cobalt nanoparticles in aqueous solutions, the formation mechanism, electronic spectra and reactions were studied.[22] Radiation-induced chemical reduction of cobalt ions from aqueous solutions of $Co(ClO_4)_2$ and HCOONa produced spherical cobalt particles with diameters of 2–4 nm. Sodium polyacrylate with a molecular mass of 2100 was used as a stabiliser. Radiolysis produced solvated electrons e_{aq}^-, hydroxyl radicals, hydrogen atoms and $CO_2^{-\bullet}$ radical ions

$$H_2O \longrightarrow e_{aq}^-, H^\bullet, OH^\bullet,$$

$$OH^\bullet(H^\bullet) + HCO_2^- \longrightarrow H_2O(H_2) + CO_2^{-\bullet}.$$

Hydrated electrons and $CO_2^{-\bullet}$ radical ions reduced Co^{2+} ions producing cobalt nanoparticles which demonstrated an absorption maximum in the 200 nm wavelength range. The use of pulse radiolysis has shown that the reduction of Co^{2+} with the formation of cobalt nanoparticles occurred by an autocatalytic mechanism.

Radiation-induced chemical reduction of Ni^{2+} ions in aqueous solutions of $Ni(ClO_4)_2$ containing propan-2-ol in the presence of polyethylene, polyacrylate and poly(vinyl sulfate) produced metal sols comprising spherical particles with diameters of 2–4 nm. Nickel nanoparticles easily oxidisable by O_2 and H_2O_2 form sufficiently stable Ni–Ag nanosystems in the interaction with silver ions.[23]

Spherical copper particles measuring 20–100 nm were obtained by γ-radiolysis of $KCu(CN)_2$ aqueous solutions in the presence of methanol and propan-2-ol as the acceptors of hydroxyl radicals.[24]

Silver particles were obtained upon γ-radiolysis of solutions of silver nitrate in water, ethanol and 0.01 M $C_{12}H_{25}OSO_3Na$.[25] The fractal dimensions of aggregates were 1.81, 1.73 and 1.70 in water, ethanol and $C_{12}H_{25}OSO_3Na$, respectively.[25] Stable nanoparticles (the average size of 1–2 nm) of platinum, rhodium and ruthenium were prepared in organic media by heating the corresponding colloidal solutions of the metal hydroxides in ethanol.[26]

Silver particles measuring 2–7 nm were obtained by electrochemical dissolution of a metal anode (silver plate) in an aprotic solution of tetrabutylammonium bromide in acetonitrile.[27] This process was shown to depend on such characteristics as the current density and the nature of the cathode material. Thus at high current densities under nonequilibrium conditions, particles of irregular shapes can be formed. In the interval from -1.35 to -6.90 nA cm^{-2}, the particle diameter changed from 6 ± 0.7 to 1.7 ± 0.4 nm. In the reduction of silver ions stabilised by tetrabutylammonium bromide, silver nanoparticles were formed and deposited on cathodes made of either platinum or aluminium (Fig. 1). The use of platinum cathodes resulted mainly in the formation of spherical silver nanoparticles, whereas only films were deposited on aluminium cathodes. An analysis of the optical spectra of nanoparticles measured during their syntheses led to the conclusion that this process includes an autocatalytic stage. It was also shown that the half-width of the surface plasmon peak of a particle linearly depends on $1/R$ (R is the particle radius) and the plasmon band shifts to lower frequencies with a decrease in the particle size.

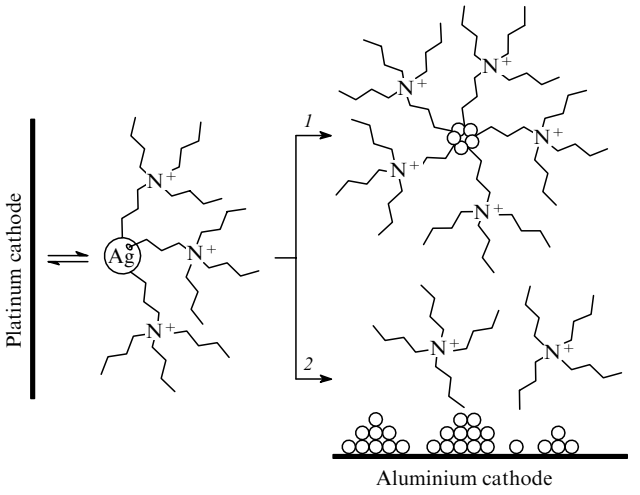


Figure 1. Schematic illustration of the competition between two processes. (*1*) Formation of silver particles and (*2*) deposition of particles and formation of a film.[27]

2. Reactions in micelles, emulsions and dendrimers

Micelles, emulsions and dendrimers,† which can be considered as a sort of nanoreactors, which make it possible to synthesise particles of definite sizes, are used for preparing metal nanoparticles. Crystalline bismuth nanoparticles measuring less than 10 nm were obtained by reduction of aqueous solutions of bismuth salts inside reverse micelles based on sodium diisooctyl sulfosuccinate (usually designated as AOT).[28] Mixing of AOT dissolved in isooctane with a certain volume of an aqueous solution of $BiOClO_4$ resulted in the formation of reverse micelles. The

† A dendrimer represents a highly branched macromolecule which includes a central core, internal repeating units and terminal functional groups. Dendrimers with small numbers of internal units exist in an 'open' form, whereas those involving large number of units form spherical three-dimensional structures. Terminal groups of dendrimers can be modified by hydroxy, carboxy and alkyl groups.

micellar solution of $NaBH_4$ was prepared in the same fashion with the same ratio $w = [H_2O]:[AOT]$. Both solutions were mixed under argon. Bismuth particles precipitated after the mixture was kept for several hours at room temperature. The liquid phase was removed *in vacuo*, and the dry residue was dispersed in toluene. According to X-ray powder diffraction and electron spectroscopy data, a dark solution thus obtained contained bismuth particles measuring 3.2 ± 0.35 nm for $w = 2$ and 6.9 ± 2.2 nm for $w = 3$. When polymers were used for the protection of crystalline bismuth particles, the particle size increased to 20 nm and further.[29]

Reduction of rhodium salts in water in the presence of an amphiphilic block copolymer of styrene with ethylene oxide and an anionic surfactant (sodium dodecyl sulfate) produced rhodium particles with diameters of 2–3 nm stabilised by the block copolymer.[30] Luminescent nanomaterials based on yttrium oxide doped with europium were synthesised using non-ionic reverse microemulsions based on poly(ethylene oxide) and other ethers.[31]

At present, an active search is directed to macromolecules that can be used as matrices in syntheses of nanoparticles. In such methods, the stabiliser molecules interact with the surfaces of metal particles and affect their growth. For example, the reduction of bivalent copper in the presence of poly(*N*-vinylpyrrolidone) produced particles with the diameters of 7 ± 1.5 nm at 11 °C and 10 ± 2 nm at 30 °C.[32] Studies on the temperature effect on the stability of preformed nanoparticles have shown that if copper particles formed at 11 °C were heated to 30 °C, their polymeric shell lost its protective properties, which enhanced aggregation and accelerated oxidation of metal particles. The opposite result was achieved by cooling to 11 °C the system formed at 30 °C. In this case, the particles do not aggregate, their sizes remain unchanged and the resistance to oxidation increases. The competition of different temperature-dependent processes is reflected not only in the stabilities of particles formed but also in their size distribution.

Photochemical reduction of Ag^+ ions in the presence of dendrimers with terminal amino and carboxy groups produced silver particles with an average diameter of ~7 nm.[33] Below, a possible mechanism of particle formation is shown.

$$Ag^+ + [\text{dendrimer}]-CO_2^- \xrightarrow{h\nu} Ag^0 + [\text{dendrimer}]-CO_2^{\bullet} \longrightarrow$$
$$\longrightarrow [\text{dendrimer}]^{\bullet} + CO_2,$$
$$Ag^+ + [\text{dendrimer}]-NH_2 \xrightarrow{h\nu} Ag^0 + [\text{dendrimer}]-NH_2^{+\bullet}.$$

The particle size can be controlled by varying the nature of the dendrimers. Currently, stabilisation of metal nanoparticles is performed in the presence of dendrimers based on polyamidoamines and their derivatives. The use of dendrimers as microreactors for the synthesis of metal nanoparticles was documented in Ref. 34. Monodispersed spherical polyamidoamine dendrimers are permeable to low-molecular reactants. Thus an addition of $HAuCl_4$ to an aqueous solution of a dendrimer with primary and tertiary amino groups results in the appearance of a protonated dendrimer with $AuCl_4^-$ as the counter-ion. Reduction of $AuCl_4^-$ anions by sodium borohydride have produced 1–5-nm gold particles. By varying either the concentration ratio (D) of $AuCl_4^-$ counter-ions to terminal amino groups or the diameter (generation) of the dendrimer, one can control the particle size. Reduction of gold ions in a dendrimer of the ninth generation (G.9) resulted in the formation of spherical gold particles with the sizes of 2.5, 3.3 and 4 nm for $D = 1:4$, $1:2$ and $1:1$, respectively. For $D = 1:1$, gold particles measuring 2, 2.5, 3.2 and 4 nm were formed in dendrimers of the G.6, G.7, G8 and G.9 generations, respectively.

Reduction of gold and silver salts in the presence of modified dendrimers produced particles with an average diameter of 2–6 nm. The autocatalytic mechanism of the reaction has been revealed using spectral methods.[35]

The prospects of using mesopores for the preparation of different nanosize materials were discussed.[36] Nanoparticles of silver and silver sulfide were obtained in nanosize cavities of perfluorinated ionomer membranes.[37] Reduction of metal ions in the presence of aminodextran and styrene resulted in the formation of spherical polystyrene particles with diameters of ~2.0 μm covered with gold and silver islets measuring from 5 to 200 nm.[38]

3. Particles of different shapes and films

The sizes and shapes of particles often depend on the synthetic methods; however, the ratio of nucleation to growth rates of particles is also of great importance. Each of these processes depends in turn on variations in the reaction conditions such as temperature, the nature and concentrations of metal and ligand and the nature of stabiliser and reductant. The problems of nucleation and particle growth are surveyed in detail elsewhere.[15]

The shapes of metal nanoparticles formed in the reduction of metal salts can be controlled using tetra-n-octylammonium carboxylates $(n\text{-}C_8H_{17})_4N^+(RCO_2)^-$ as the reductants and stabilisers (see Ref. 39). Palladium particles measuring 1.9 and 6.2 nm were formed in the reaction

$$Pd(NO_3)_2 + (n\text{-}C_8H_{17})_4N^+(RCO_2)^- \xrightarrow{\text{THF, 66 °C}} \text{Pd particles.}$$

Their sizes and shapes were determined by electron microscopy. It was found that if acetate, dichloroacetate, pivalate or pyruvate anions were used, the particles formed had largely spherical shape. However, if palladium nitrate was treated with an excess of $(n\text{-}C_8H_{17})_4N^+(HOCH_2CO_2)^-$, triangular particles with an average size of 3.6 nm were formed in addition to spherical ones. The shape changes observed were attributed [39] to the presence of the hydroxy group in the anion.

A nickel compound $Ni(COD)_2$ (COD is cycloocta-1,5-diene) was used for elucidating the role (reductant or stabiliser) the glycolic acid residue plays in the reduction.[39] The reaction was as follows:

$$Ni(COD)_2 + (n\text{-}C_8H_{17})_4N^+(HOCH_2CO_2)^- \xrightarrow{H_2,\ 60\ °C} \text{Ni particles.}$$

Inasmuch as nickel in $Ni(COD)_2$ is in its zerovalent state, the glycolate can act only as a stabiliser, whereas it is hydrogen that reduces COD to cyclooctane. By means of electron microscopy it was found that the reaction produces crystalline nickel particles with an average size of 4.5 nm preferentially shaped as triangles. In control experiments using $(n\text{-}C_8H_{17})_4N^+Br^-$ or $(n\text{-}C_8H_{17})_4N^+NO_3^-$ as stabilisers, spherical particles were formed. The triangular shape of particles was additionally confirmed by the results of scanning tunnelling microscopy. The glycolate effect on the morphology of particles formed seems to be associated with the selective adsorption of anions on growing nanocrystals, which can be traced by changes in the absorption spectra. During synthesis of nanoparticles, the band at 1621 cm^{-1} which belongs to dissolved glycolate disappears, and a new band appears at 1604 cm^{-1}, which corresponds to adsorbed glycolate. It is believed [39] that the changes observed in the IR spectra recorded *in situ* agree with the proposed mechanism.

The formation of spherical and cylindrical silver nanoparticles was observed upon photochemical reduction of silver salts in the presence of polyacrylic acid.[40,41] Polyacrylic acid and Ag^+ ions form a complex which, being illuminated, produces silver nanoparticles. According to electron microscopy and sedimentation analysis data, photoreduction of the complex produced spherical silver nanoparticles measuring 1–2 nm. In the presence of a modified (partially decarboxylated) acid, apart from spherical particles, elongated particles (nanorods) with lengths of up to 80 nm characterised by light absorption in the 500–800-nm range were also formed. Apparently, decarboxylation disturbs the cooperative mechanism of the bonding between polyacrylic acid and

silver cations, making the stabilisation of spherical particles less effective and favouring the growth of nanorods.

The sizes of metal particles formed in the presence of macromolecular stabilisers depend on the conditions of formation of the polymeric protective shell. If the polymer involved is an insufficiently effective stabiliser, a particle already bound to the macromolecule may continue to grow. Changing the monomer and the corresponding polymer and varying the polymer concentration in solution, enables one to control the sizes and shapes of particles formed.

An original method of changing the stabilising ability of a polymer was proposed.[42] The authors studied how the conformation of poly(*N*-isopropylacrylamide) affected the shape of platinum nanopartilcles formed upon the reduction of K_2PtCl_4 by hydrogen. This polymer can change its conformation with temperature. Below 306 K, polymer molecules are hydrophilic and represent swelled globules; in this case, up to 60% of platinum nanoparticles formed have irregular shapes. At temperatures above 306 K, polymer molecules are hydrophobic and begin to collapse. The stabilising ability of such molecules decreases. At 313 K, the reduction of platinum ions proceeded on the most active (111) face of the growing nanocrystal, and cubic nanoparticles were preferentially formed (in up to 68% yield). The morphology of the particles also depended on the concentration ratio of platinum salt and polymer in solution (however, to the lesser extent than on the temperature).

The shapes and sizes of silver nanoparticles can be controlled when the methods of pulse sonoelectrochemistry (the use of ultrasound in electrochemistry) were applied.[43,44] Ultrasound allows one to clean and degasify the electrode surface, accelerate mass transfer and increase the reaction rate. Silver particles shaped as spheres, rods and dendrites were obtained by the electrolysis of aqueous solutions of $AgNO_3$ in the presence of $N(CH_2COOH)_3$. These were characterised by electron microscopy, X-ray diffraction and electron spectroscopy. The shapes of particles were found to depend on the reagent concentration. Spherical particles had diameters of $\sim$20 nm. The diameters of rods were 10–20 nm. In certain cases, their surfaces exhibited protrusions which could be developed into dendrites.

An interesting method of successive layer-by-layer deposition of thin (100–300 nm) films incorporating magnetic nanoparticles was considered.[45] Alternating layers of magnetic nanoparticles, *e.g.*, Fe_3O_4, and poly(diallyldimethylammonium bromide) were first deposited on a glass plate covered with paraffin and acetyl cellulose. Upon reaching the desirable film thickness, the cellulose layer was removed, and the whole specimen was dissolved in acetone. The suspension thus obtained could be applied on any porous surfaces and dense supports. It was noted that the films which incorporate uniform magnetic nanoparticles measuring $\sim$10 nm, can be used in memory devices.[46]

At present, the control over the shapes and sizes of nanoparticles seems to be the most important problem of nanochemistry.[47] Synthesis of uniform spherical and rod-like particles of metallic iron have been described.[48] Nanoparticles were prepared by thermal decomposition of iron pentacarbonyl in the presence of stabilisers. Spherical particles measuring 2 nm were uniformly dispersible in solution and formed rods of 2-nm diameters and 11-nm lengths. These particles were amorphous, whereas the rods had the face-centred cubic structure of α-iron.

Different supports with films of 4-mercaptobenzoic acid applied in high vacuum were used for the preparation of thin heterogeneous films with incorporated nanoparticles of gold, silver, and cadmium sulfate. The heterogeneous films were synthesised by successive immersion of supports in the corresponding solutions.[49]

High-resolution electron microscopy has shown that, being encapsulated into micelles, rod-like gold nanoparticles prepared by an electrochemical method grow along the [001] axis. Here, (100) faces of the particles remain stable, whereas (110) faces are unstable.[50]

The possibility of structural changes in platinum nanoparticles supported on silicon and the microcrystalline structure of individual nanoparticles were studied by electron microscopy before and after the system was heated *in vacuo* and in hydrogen and oxygen atmospheres.[51] In all the cases, the mass of particles remained unchanged, but the sizes of constituent crystals increased with temperature. This was attributed to surface fusion and self-diffusion of platinum particles. Studies of adhesion of platinum particles to silica which were carried out using atomic force microscopy have shown that heating changes the crystalline nature of particles and strengthens their adhesion to silica. Moreover, platinum nanoparticles were shown to be stable both under oxidative and reductive conditions.

4. Reactions of oxides

Like metals, oxides also find extensive application in practice. The reactivity of metal oxides is low compared with the corresponding metals; therefore, oxide formation is used for stabilising metal nanoparticles. Recently, metal oxide nanoparticles have been employed in reactions which are of interest for nanochemistry.

An original application of nanocrystalline zinc oxide has been described,[52] where zinc oxide was synthesised by a modified sol–gel method by the reactions

$$ZnEt_2 + 2\,Bu^tOH \longrightarrow Zn(OBu^t)_2 + 2\,C_2H_6,$$

$$Zn(OBu^t)_2 + 2\,H_2O \longrightarrow Zn(OH)_2 + 2\,Bu^tOH,$$

$$Zn(OH)_2 \longrightarrow ZnO + H_2O.$$

The process of ZnO preparation involved three stages: synthesis, isolation and activation. The latter process, in turn, consisted of several successive stages of thermal treatment. First, the powder was slowly heated to 90 °C and kept at this temperature for 15 min. Then, the temperature was gradually increased to 250 °C, held at this level for 15 min and slowly decreased to room temperature. Zinc oxide thus obtained represented crystalline nanoparticles measuring 3–5 nm with a surface area of $\sim$120 $m^2\ g^{-1}$. Nanosize zinc oxide was used in the reaction

$$2\,ZnO + CCl_4 \longrightarrow CO_2 + 2\,ZnCl_2.$$

The process was carried out at 250 °C, and CCl_4 was introduced into the reaction vessel portionwise at 7-min intervals. Carbon dioxide and nonconsumed CCl_4 were quantitated by gas chromatography. Nanocrystalline zinc oxide was shown to be more reactive than common commercial specimens. It was also shown that the adsorption of sulfur dioxide and the destructive adsorption of diethyl 4-nitrophenyl phosphate (a noxious organophosphorus compound) proceed with a higher efficiency on nanocrystalline zinc oxide.[52] In these processes, nanocrystalline ZnO exhibited higher reactivity compared with commercial specimens.

Nanocrystalline oxides of alkali-earth metals were successfully used for deactivation of yperite (mustard gas) and other war gases. Autocatalytic dehydrohalogenation of 2,2′-dichlorodiethyl sulfide on nanocrystalline calcium oxide was studied using NMR technique.[53] The decomposition products of 2,2′-dichlorodiethyl sulfide were found to involve divinyl sulfide ($\sim$80%) and thioglycol and/or a sulfonium ion ($\sim$20%) with a hydroxyalkyl group, which seem to provide its binding to the surface of the alkali-earth metal oxide. In addition to the reaction of CaO with yperite, its reactions with organophosphorus compounds were studied. The kinetics of the reactions of all studied substances with calcium oxide was shown to be characterised by a rapid initial stage followed by a slow diffusion-controlled stage.

An interesting application of transition metal oxides has been discussed.[54] Particles of cobalt, nickel, copper and iron oxides measuring 1–5 nm were used as the electrode materials in lithium power sources (electrochemical capacity of 700 $\mu A\ h\ g^{-1}$). Here, the formation and decomposition of Li_2O and the accompanying reduction and oxidation of nanoparticles occur on electrodes

made of CoO nanoparticles. The scheme of reversible reactions is as follows:

$$2\,Li - 2e^- \rightleftharpoons 2\,Li^+$$
$$CoO + 2\,Li^+ + 2e^- \rightleftharpoons Li_2O + Co$$
$$CoO + 2\,Li \underset{2}{\overset{1}{\rightleftharpoons}} Li_2O + Co$$

The direct reaction (*1*) is possible and thermodynamically permissible. The reverse reaction (*2*) is unusual for electrochemistry, because Li_2O is traditionally considered to be electrochemically inactive. Electrochemical decomposition of Li_2O using mechanically ground Li_2O and CoO powders could not be effected.[54] Thus, the possibility of the reverse reaction is associated with the use of nanoparticles and the increase in their electrochemical activity with a decrease in size.

Currently, great attention has been drawn to the preparation and analysis of physicochemical properties of hybrid nanomaterials of the core–shell type and the particles which involve two and even three different metals.

New nanocrystalline hybrid core–shell materials such as TiO_2-MoO_3 were prepared and studied in detail.[55] The $TiO_2-(MoO_3)_x$ particles were synthesised by co-nucleation of metal oxides on the surfaces of micelles.

In such materials, the photoabsorption energy correlates with the particle size. With a decrease in the sizes of TiO_2-MoO_3 particles from 8 to 4 nm, the absorption energy decreased from 2.9 to 2.6 eV. For comparison, it may be noted that the forbidden gap energies of bulk TiO_2 and α-MoO_3 are 3.2 and 2.9 eV, respectively. Unfortunately, the materials obtained turned out to be less efficient in photocatalysed oxidation of acetaldehyde compared with common titanium dioxide produced by Degussa (France).

To facilitate the electron transport in metal nanoparticles, it was proposed to use the pH-induced changes in the charges of stabilising shells which are bound to the particle surface. Molecules of rigid mercaptophenylacetylenes were shown to bind strongly gold and silver particles.[56] It was found that electron transport in charged gold particles is better described in terms of classical rather than quantum-mechanical concepts.[57]

The use of nanoparticles of metals and their oxides in optical and electronic devices requires that new approaches be found to the solution of such problems as: establishment of reliable electrical contacts between individual nanoparticles; determination of characteristics of electromagnetic interactions between particles in symmetrical well-organised aggregates of nanoparticles; elucidation of how the chemical properties of the surface of nanoparticles depend upon their size and its effect on their optical and electronic properties.[58]

5. Bi- and trimetallic particles

Nanoparticles that involve two or more different metals are of particular interest for the development of materials with novel properties, because at the nanolevel it is possible to synthesise such intermetallic compounds and alloys that can never be formed for bulk specimens.

Nanoparticles involving two[59] and even three[60] different metals were obtained by radiation-induced reduction of salt solutions. A two-step synthesis was used for the preparation of Au–Hg particles. First, radiation-induced reduction produced 46-nm gold particles. Then, $Hg(ClO_4)_2$ and propan-2-ol were added to the gold sol, which resulted in deposition of mercury ions on the gold particles. Finally, mercury ions were reduced by free radicals formed upon radiolysis.

Palladium particles measuring 4 nm with a narrow size distribution were prepared by the reduction of Na_2PdCl_4 by hydrogen in the presence of sodium citrate. The addition of $K_2Au(CN)_2$ to the sol of palladium particles in methanol followed by γ-irradiation resulted in the reduction of gold ions. No individual gold particles were formed: all gold was deposited on palladium particles and formed an outer layer. A silver layer could also be deposited on the Pd–Au particles obtained. These multilayer clusters seem to be of interest for studying rapid (femtosecond) electronic processes.[61,62]

The use of silicates modified by organic compounds as matrices and stabilisers made it possible to synthesise bimetallic nanoparticles, their sols and gels by a single-step method.[63] Scanning tunnelling microscopy studies of Pd–Pt particles have shown the latter to consist of palladium cores covered with platinum shells. Thin silicate films with bimetallic nanoparticles were used in electrocatalytic oxidation of ascorbic acid.

A sonochemical method was applied to produce bimetallic gold–palladium nanoparticles.[64] The particles were synthesised in aqueous solutions of $NaAuCl_4 \cdot 2H_2O$ and $PdCl_2 \cdot 2NaCl \cdot 3H_2O$ with sodium dodecyl sulfate added. The latter functioned as both the stabiliser and the reductant. The bimetallic particles synthesised represented cores of gold atoms surrounded by shells of palladium atoms. The sizes of cores and shells were measured for different gold to palladium ratios using high-resolution electron microscopy. The use of X-ray spectroscopy allowed the gold and palladium contents in the particles to be determined. With the known density, mass and initial ratio, one can estimate the sizes of cores and shells (Table 1). Using the sonochemical synthesis of bimetallic particles, one can control the sizes of cores and shells by varying Au^{3+} and Pd^{2+} concentrations. Bimetallic Au–Pd particles exhibited high catalytic activity in hydrogenation of pent-4-enoic acid.

Table 1. Core diameter (gold) and shell thickness (palladium) in Au–Pd bimetallic nanoparticles.

Au : Pd ratio	Experiment		Estimate	
	core diameter	shell thickness	core diameter	shell thickness
1 : 1	6.0	1.0	6.4	0.8
1 : 4	5.0	1.5	4.8	1.6

A comparative study of gold, nickel and bimetallic Au–Ni nanoparticles on amorphous carbon supports, which were obtained by laser ablation of the corresponding pure metals and the alloy, was carried out.[65] Studies accomplished by different methods have shown the bimetallic particles to have, on average, diameters of 2.5 nm and a narrow size distribution, while their composition was found to correspond to that of the evaporated alloy.

Nanoparticles of FeTiH were prepared by mechanical synthesis from a mixture of iron and titanium hydride.[66] Nanosize iron–tungsten composite particles with a tungsten concentration varying from 2 at.% to 85 at.% were synthesised by coreduction of a mechanical mixture of iron hydroxide ($FeOOH \cdot nH_2O$) and tungstic acid (H_2WO_4) in a flow of hydrogen at 740 °C for 1 h. The particles obtained were studied by X-ray diffraction and Mössbauer spectroscopy.[67]

III. Cryonanochemistry of metals

The presence of stabilisers, the size distribution of nanoparticles, their different shapes and the interactions between nanosize particles and the medium complicate the studies of the reactions involving metal nanoparticles. In addition, high chemical activities of metal atoms and nanoparticles they form require special approaches to their studies to be developed. One of such approaches is isolation of nanoparticles at superlow temperatures (4–10 K) in inert-gas matrices. Co-condensation of a large amount of an inert gas, *e.g.*, argon, and a small number of nanoparticles (more than 1000 inert gas species per metal particle) allows active particles to be effectively isolated from one another,

while low temperatures hinder diffusion of these particles and provide their stabilisation in an inert matrix.

Here, we will not analyse all the studies devoted to reactions of metal atoms and the corresponding nanoparticles at low and superlow temperatures and only consider the results of recent publications.[68–70] The specimens under discussion were prepared by co-condensation of vapours of metals and ligands on surfaces cooled either to 10 or 77 K. In certain experiments, the vapours were diluted by argon. The amount of metal deposited was determined using quartz-crystal microbalances. The co-condensates obtained were studied by spectroscopy in UV, visible and IR ranges. ESR spectroscopy was also used. Table 2 lists the products formed upon reactions of magnesium and samarium particles with different ligands in argon matrices at 10–40 K.[68,69]

Table 2. Reaction products of samarium and magnesium particles with different ligands in an argon matrix at 10–40 K.

Metal	Ligand		
	CO_2	C_2H_4	CH_3X (X = Cl, Br)
Mg	$Mg^+CO_2^-$, upon annealing of the matrix	cyclic $Mg(C_2H_4)_2$ (see Fig. 2 *a*), upon annealing of the matrix	CH_3MgX, upon irradiation ($\lambda > 280$ nm for Mg and $\lambda > 300$ nm for Mg_{2-4} and Mg_x)
Mg_{2-4}	$Mg^+CO_2^-$, upon co-condensation		
Mg_x	$Mg^+CO_2^-$, upon annealing of the matrix		
Sm	$Sm^+CO_2^-$, CO, $SmCO_3$, upon annealing of the matrix	$Sm(C_2H_4)$ and $Sm(C_2H_4)_2$ complexes	methane, upon co-condensation
Sm_2, Sm_x	$Sm^+CO_2^-$, CO, $SmCO_3$, upon co-condensation		

Studies of properties of metal nanoparticles, in particular at low temperatures, face various difficulties. Therefore, theoretical simulation of the structures of metal nanoparticles, their electronic, optical and other properties and the processes of their aggregation is gaining in importance.

In theoretical studies of nanoparticles, valuable results can be obtained by *ab initio* quantum-chemical calculations which use the concepts developed by solid-state physics, and by calculations based on the molecular dynamics approach. At present, the Hartree–Fock method is applied for the determination of properties of atoms and small clusters. Particularly, this method was successfully employed for the calculation of the properties of nickel particles which involved $n = 4$, 6, 8 and 13 atoms.[71] The density functional method is also widely used for the simulation of the behaviour of metal nanoparticles.[13] For example, the latter method was used for studying the structure and properties of Pt_{13} and Pt_{55} species.[72] The results obtained were also compared with those of different *ab initio* and semi-empirical quantum-mechanical methods which are used in calculations of properties of metal nanoparticles. The density functional method was applied[73] for studying the products of carbon monoxide adsorption on palladium particles deposited on magnesium oxide. An extended Hückel method was used for studying bimetallic nanoparticles of Pt–Fe alloys with a number of atoms ranging from 13 to 309.[74]

The *ab initio* quantum-mechanical calculations have shown that the magnesium–carbon dioxide system represents a metastable $Mg^+{}^{\bullet}CO_2^{-\bullet}$ radical-ion pair. According to calculations, this pair is stabilised by the argon matrix. The IR spectrum of the argon–ethylene co-condensate have revealed absorption bands of ethylene dimers. As was shown by calculations, the potential

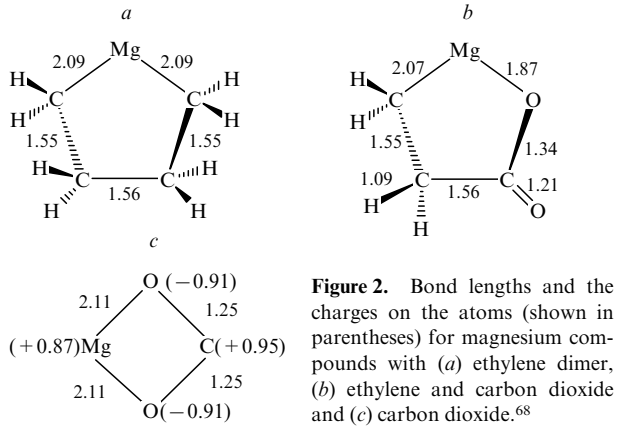


Figure 2. Bond lengths and the charges on the atoms (shown in parentheses) for magnesium compounds with (*a*) ethylene dimer, (*b*) ethylene and carbon dioxide and (*c*) carbon dioxide.[68]

surface of the $Mg \cdot 2C_2H_4$ complex demonstrates no global minimum corresponding to the C_{2v} symmetry. The global minimum can be obtained if only all the restrictions on the system's symmetry are removed. In the Møller–Plessett (MP2) approximation, the minimum corresponded to a cyclic structure which involves an ethylene dimer and a magnesium atom. The interatomic distances in the structures of magnesium complexes with ethylene and carbon dioxide were calculated. Figure 2 shows the structures of these complexes.

Studies of a samarium–carbon dioxide co-condensate have shown that samarium and CO_2 form a complex with an angular structure. In the reaction products, CO and CO_3^{2-} were detected. Radical anions $CO_2^{-\bullet}$ and a samarium carbonyl compound of an uncertain composition were also formed. Figure 3 shows the data on the reaction products identified and on their interconversions. Figure 4 shows the temperature dependence of the relative activity of samarium nanoparticles in the reaction with CO_2. The results

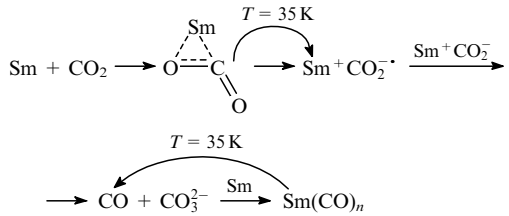


Figure 3. Schematic illustration of the reactions of samarium atoms with carbon dioxide molecules in an argon matrix. Straight arrows are the reactions occurring during co-condensation; curved arrows are the reactions occurring during heating of the co-condensate.[68]

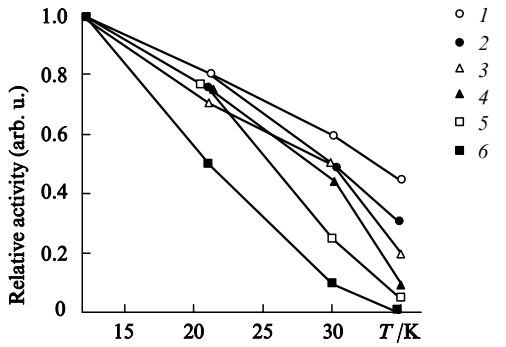


Figure 4. A temperature dependence of the relative activity (in arbitrary units) of samarium atoms and nanoclusters in the reaction with carbon dioxide.[9] (*1*) Sm, $\lambda = 501$ nm; (*2*) Sm, $\lambda = 557$ nm; (*3*) Sm, $\lambda = 520$ nm; (*4*) Sm_x, $\lambda = 641$ nm; (*5*) Sm_x, $\lambda = 600$ nm; (*6*) Sm_2, $\lambda = 541$ nm (λ is the wavelength in the electronic spectrum).

shown suggest a higher activity of samarium nanoparticles compared with samarium atoms. A similar trend was observed for magnesium nanoparticles. According to IR spectroscopic data, in samarium – ethylene co-condensates, 'sandwich' π-complexes of samarium and ethylene SmC_2H_4 and $Sm(C_2H_4)_2$ are formed rather than cyclic compounds typical of magnesium co-condensates.

At ordinary temperatures, the reactions of bulk magnesium and samarium with alkyl halides occur in a similar way to give organometallic compounds. At low temperatures, atoms and small clusters of these metals react with haloalkanes (*e.g.*, with halomethanes) by different routes. Magnesuim inserts into the C – Br and C – Cl bonds with the formation of Grignard reagents, whereas samarium, being more reactive, reduces CH_3Cl and CH_3Br to methane. Thus, on the nanoparticle level, magnesium and samarium behave differently.

Another peculiarity in the behaviour of magnesium and samarium nanoparticles was observed in their reactions with mixtures of two ligands, *viz*., CO_2 and C_2H_4. It was found that under comparable conditions magnesium and samarium react only with CO_2 and do not react with ethylene. The results obtained demonstrate that no unambiguous relationship exists between the activity and selectivity of metal nanoparticles.

The formation of complexes and organometallic nanostructures was studied by an example of film co-condensates of the vapours of metallic silver and mesogenic cyanobiphenyls $C_nH_{2n+1}C_6H_4C_6H_4CN$ ($n = 5$ and 8) and $C_nH_{2n+1}OC_6H_4.C_6H_4CN$ ($n = 8$) in the temperature interval of 80 – 350 K.

Low-temperature co-condensation of silver particles with $C_5H_{11}C_6H_4C_6H_4CN$ and $C_8H_{17}C_6H_4C_6H_4CN$ produced π-complexes stable at low temperature.[68] IR and UV spectroscopic studies have confirmed their formation and revealed their sandwich structures and 1 : 2 composition; 1 : 1 complexes were also detected. The structure of π-complexes determined from IR spectroscopic data was confirmed by model quantum-chemical calculations.[75] Vibrational frequencies of CN groups were also calculated and compared with the experimental ones. Spectral properties of the reaction products of mesogenic cyanobiphenyls with silver particles were discussed in detail elsewhere.[76]

Thermal degradation the complexes undergo on being heated to the room temperature results in the formation of nanosize (15 – 30 nm) silver clusters and their subsequent aggregation with formation of anisotropic particles (more than 200 nm long) stabilised in a liquid-crystal line matrix.[76] An analysis of the ESR spectrum of a co-condensate of silver particles with 4-pentyl-4′-cyanobiphenyl at 90 K has revealed two spectral doublets. The values of the *g*-factor and the hyperfine coupling constant (*a*) for ^{107}Ag and ^{109}Ag are as follows: $g(^{107}Ag) = 2.001$, $a(^{107}Ag) = 48.5$ mT and $g(^{109}Ag) = 2.003$, $a(^{109}Ag) = 72.75$ mT. The occupation degree (ρ_m) of valence *s* orbitals of the metal in the complex was estimated ($\rho_m = 0.77$). The value obtained suggests that electron density is shifted from a silver atom to the π-orbitals of the ligand. The ESR spectrum also revealed a broad anisotropic singlet which was tentatively attributed to zero-valent silver nanoparticles.

Optical spectroscopy in the UV and visible ranges in combination with the dynamic light scattering technique were used for studying the properties of polymer-stabilised silver nanoparticles.[77] Co-condensation of vapours of silver and 2-dimethylaminoethyl metacrylate *in vacuo* occurred on the walls of a glass vessel cooled by liquid nitrogen. According to the electron microscopic data, heating of the co-condensate to room temperature resulted in the formation of polymer-stabilised silver nanoparticles measuring 5 – 12 nm. Dynamic light scattering studies have shown that the size distribution of these particles is bimodal. Such a distribution seems to suggest that both isolated silver particles and their aggregates are simultaneously present in the system. The dependence of the radius of a solvated particle on the nature of the solvent was studied. Among the solvents such as water, toluene and acetone, the latter gave solutions containing silver particles with the smallest radii.[78]

Co-condensation of lead and a monomer polymerisable at low temperatures, *viz*., *p*-xylylene, vapours at 80 K, afforded films with incorporated lead nanoparticles. Conductivity of the films was studied in the course of co-condensation and subsequent heating.[79] The metal – polymer films obtained exhibited satisfactory sensor activity with respect to ammonia in air and ammonia in the presence of water vapour.

Complexes of zero-valent samarium with 1,3,5-tri(*tert*-butyl)-benzene were obtained by co-condensation of metal and ligand vapours at 80 K. Kinetics of thermal decomposition of these complexes was studied.[80,81] Transformations that occur in samarium complexes with mesogenic cyanobiphenyls were also studied at low temperatures.[82] It was shown that the complex with the composition $Sm : C_5H_{11}C_6H_4C_6H_4CN = 1 : 2$ transforms in the temperature range 170 – 210 K into the complex $Sm : C_5H_{11}C_6H_4C_6H_4CN = 1 : 1$; this reaction is characterised by an effective activation energy of 8 kJ mol^{-1}. The reaction of magnesium particles with chloro-, bromo- and iodobutanes at low temperatures was studied.[83] It was shown that the yield of octane (the Würtz reaction product) depends on the amount of magnesium and the carbon – halogen binding energy. The mechanism of the reaction of magnesium with alkyl halides and the earlier data on the cryonanochemistry of metal particles have been discussed elsewhere.[2,3]

IV. Ensembles involving nanoparticles

When metal nanoparticles are synthesised by the condensation method, the process begins with the formation of nanoparticles of individual metal atoms; this may be considered as 'self-assembly' or 'self-organisation'‡ of atoms with the formation of atomic ensembles.

As applied to metal nanoparticles, it is common practice to consider both the ensembles of particles themselves and the ensembles of stabilising protective layers. Prime attention is given to the effect of the chemical nature of stabilisers on self-assembly processes. An analysis of studies devoted to self-assembly and performed before 2000 is given elsewhere.[13] The synthesis of thiol-covered metal particles and their self-assembly into one-, two- and three-dimensional superlattices were surveyed in Ref. 85.

The processes of assembly and self-assembly of nanoparticles were discussed most extensively by the example of silver and gold nanoparticles. Monodispersed silver nanocrystals were stabilised by chemisorption of dodecanethiol on the receptor sites of the crystal surface.[86] The kinetics of aggregation and the structure of the formed ensembles of stabilised particles depend on the number of receptors on the nanocrystal surface.

The formation of alternating positively charged gold particles and negatively charged silver particles and their self-assembly in the presence of 4-mercaptoaniline and 4-mercaptobenzoic acid on a glass surface were described.[87] One-dimensional layers of gold particles on silicon supports were also formed.[88] The latter process was realised using atomic force microscopy (AFM) for surface treatment and chemical deposition of gold particles.

Self-assembly of gold particles measuring 4.6 nm results in aggregates with diameter of ~30 nm.[89] The initial gold particles were prepared by the reduction of $HAuCl_4$ by $NaBH_4$ in the presence of $HSCH_2COONa$. Removal of the excess metal ions from the solution by dialysis resulted in the formation of coarser aggregates. Before the dialysis, the electronic spectra of particles revealed no plasmon peak typical of gold particles.

A method of synthesising materials from 'bricks and mortar' was first described in Ref. 90. Binding between a polymer and

‡ General description of such self-organisation is given in a monograph by Lehn.[84]

thymine-protected gold particles was provided by hydrogen bonds formed. The process of self-association of particles into aggregates, the sizes of the aggregates and their morphology were temperature-controlled. At 23 °C, the initial 2-nm gold nanoparticles formed spherical aggregates with diameter of 97 ± 17 nm. At -20 °C, spherical aggregates with diameter of 0.5 – 1 μm, which in turn comprised finer aggregates as individual subunits, were formed. At 10 °C, ~50-nm-long chains built of spherical nanoparticles were formed. These self-association processes were studied using X-ray small-angle scattering and transmission electron microscopy (TEM). It was assumed that the formation of aggregates at 10 °C is an intermediate stage of the formation of coarser ensembles at -20 °C, and the former aggregates can be used as the precursors of nanoensembles of different shapes and sizes.

Self-assembly of rod-like gold particles with diameter of 12 nm and lengths of 50 – 60 nm was studied using high-resolution electron microscopy.[91] By choosing concentrations of these particles, their size distribution, the conditions of solvent evaporation, its ionic strength and the surfactant concentration, one-, two- and three-dimensional structures can be obtained by electrolysis. A mixture of hexadecyltrimethylammonium bromide and tetraoctylammonium bromide was used as the water-soluble electrolyte. Tetraoctylammonium bromide provided the formation of cylindrical particles, where the ratio of two surfactants determined the diameter to length ratio of the gold nanorods formed. The electrolysis was carried out for 4.5 min. Gold nanorods were formed on a copper wire net partially immersed in solution (on net – solution contacts). Presumably, the following two factors are most important for further self-assembly of the rods, *viz*., the induced convective transfer of particles from the solution to the thin film by evaporation of water and the interaction of particles within the film, which results in the formation of different structures.[91] A possible reason for the parallel arrangement of rod-like particles is associated with capillary forces that act between parallel rods, although more accurate theoretical analysis is required to explain the anisotropy of the rod ensembles observed.

Self-assembly of nanoparticles entails not only the translational ordering but also the orientational one. The orientational ordering is typical of particles with well determined shapes.[92] Structural changes in gold nanorods upon the action of femtosecond and nanosecond laser pulses were studied by high-resolution electron microscopy.[93] The energy of a pulse did not exceed the value necessary for melting the rods but was sufficient for inducing deformational processes which caused changes in the shapes of nanoparticles: a transition of nanorods into nanospheres was observed. The size and shape distributions of nanorods before and after their exposure to a laser beam were statistically analysed.[94]

In connection with the problem of the development of electronic nanodevices, the problem of synthesising nanoparticles protected by monolayers has attracted attention. The methods of preparation of such layers on gold particles by using solutions of hexanethiols and hexanedithiols in organic[95] and aqueous[96] media were developed.

Stable gold films which involved particles measuring ~4 nm were prepared[97] by the reaction of low-molecular-weight ($M \leqslant 4000$) polymers (such as polyethylenimine and poly-L-lysine) with gold particles covered with carboxylic acids. The film morphology was shown to depend on the nature of the acid which covers the particles. The use of mercaptododecanoic and mercaptosuccinic acids has provided films with higher degrees of ordering.

Glass-supported thin porous gold films were prepared using colloidal gold crystals as the templates. These films were studied by scanning tunnelling microscopy.[98, 99]

Microstructures, wettabilities and thermal stabilities of self-assembly manolayers of partially fluorinated alkanethiols of the $F(CF_2)_{10}(CH_2)_nSH$ (n = 2, 6, 11, 17, 33) type on gold particles were studied.[100] Introduction of fluorocarbon chains as the terminal groups into alkanethiols enhanced the stability of self-assembly manolayers (a gold-supported monolayer of non-fluorinated alkanethiols loses its ordering at ~100 °C). Fluorinated compounds with the numbers of methylene groups in a chain n = 11, 17, 33 formed well ordered monolayers. For smaller numbers of methylene units, the degree of ordering decreased. Wettabilities of the layers were also shown to depend on the number of methylene units. Thermal stabilities of self-assembled gold monolayers increased with an increase in n, and for n = 33 the monolayer films formed remained stable in air at 150 °C for 1 h.

The effect of the nature of the support on the morphology of two- and three-dimensional superlattices formed by dodecanethiol-covered silver sulfide nanocrystals of sizes of 5.8 nm were studied.[101] Oriented pyrolylic graphite and molybdenum disulfide were used as the supports. The self-assembly process was monitored by scanning electron microscopy and AFM. It was found that self-assembly into superlattices depends on the nature of the support and is governed, in addition to capillary forces, by van der Waals interactions of the particle – particle and particle – support types.

Self-assembled monolayers of 4′-hydroxy-4-mercaptobiphenyl, 4-(4-mercaptophenyl)pyridine and their mixtures with 4′-methyl-4-mercaptobiphenyl were deposited on the (111) faces of gold crystals and used as the templates for growing glycine crystals.[102] The morphology of glycine crystals obtained depended on the properties of supporting surfaces and was determined by hydrogen bonds formed between glycine molecules in the growing layer and functional groups on the self-assembled monolayer. Hydrogen bonds formed between the CO_2^- and NH_3^+ groups of glycine and a hydroxy group on the surface of a monolayer comprised of $HOC_6H_4C_6H_4SH$ molecules was assumed to be stronger than the interaction between the NH_3^+ group of glycine and the nitrogen atom of pyridine on the surface of a monolayer built of $NC_5H_4C_6H_4SH$ molecules.

As a rule, self-assembly of monolayers of different substances on metal nanoparticles and films was studied using X-ray photoelectron spectroscopy, ellipsometry and diffraction techniques. Electronic spectroscopy was successfully used [103] in studying self-assembly of monolayers of metalloporphyrins and metallophthalocyanines on ultrathin gold films. Gold films 1.3 – 10-nm thick were prepared using high-vacuum evaporation on mica at low temperatures. The deposition rate was varied in the range 0.2 – 0.4 A s^{-1}. The films were annealed at 250 °C for 2.5 – 4 h. The resulting films were studied using scanning atomic force microscopy, electronic spectroscopy and X-ray diffraction techniques. It was shown that isolated structurised islets were formed on the mica surface the sizes and optical properties of which were governed by the conditions of evaporation and subsequent annealing. The electronic spectra of such films demonstrated a peak due to a gold surface plasmon with a wavelength shifting from 606 to 530 nm as the thickness of the film decreased from 10 to 1.3 nm. The kinetic data on the light absorption were used for making semiquantitative estimates of the nature of bonding and chemical and structural properties of the monolayers. It was shown that the absorption in the region of the gold surface plasmon band, which is caused by association of molecules of organometallic compounds on gold films, may be used for monitoring molecules devoid of chromophore groups.

In addition to the sodium salt of AOT, its derivatives with other metals were used as the templates for self-assembly. To correctly interpret the template effect on the self-assembly of metal particles, phase diagrams of such systems are necessary.[104] By the example of the $Cu(AOT)_2 - iso\text{-}C_8H_{18} - H_2O$ system used as a template, it was shown that the shapes of nanocrystalline particles can be dramatically changed under the effect of various salts in small concentrations.[105]

The development of methods for synthesising metal nanoparticles of controllable sizes is of great interest. Apparently, the

majority of studies in this direction employed thiolates and were devoted to the preparation of gold nanoparticles. The use of alkanethiol monolayeres made it possible to synthesise gold particles stable both in solution and in the 'dry' state. Introduction of functional groups in alkanethiols [57] extended the possibilities of such a synthesis.

In the presence of alkanethiols, the formation of gold nanoparticles and the appearance of a protective layer proceed in two steps [106]

$$AuCl_4^- \text{ (in toluene)} + RSH \longrightarrow (Au^{I}SR)_n \text{ (polymer)},$$

$$(Au^{I}SR)_n + BH_4^- \longrightarrow Au_x(SR)_y .$$

This reaction combines the processes of nucleation and passivation. An increase in the RSH : Au molar ratio and the addition of the reductant at the earlier stage result, on average, in the formation of particles with smaller metal cores. A short interruption of the reaction favours the formation of thicker coatings with very small cores (< 2 nm).

The dynamics of growth of gold cores in the presence of protective monolayer coatings was studied.[106] The use of transmission electron microscopy made it possible to monitor slow changes in the sizes of gold particle cores which followed the active initial stage of the reaction. Thus it was found that with hexanethiol as the stabilising coating, the core size of a particle based on gold atoms increased to 3 nm during the first 60 h of the reaction and then remained unchanged. The knowledge of the mechanisms of growth and annealing of nanoparticles will allow one to refine the methods for synthesising finer particles with narrower size distributions.

V. Photochemistry and nanophotonics

Recently, studies which deal with kinetics and dynamics of reactions that involve metal nanoparticles have appeared. A photochemical reaction which involves n-dodecanethiol-covered silver nanoparticles dispersed in cyclohexane was studied in a picosecond time interval.[107] Figure 5 schematically shows the photoreaction mechanism.

According to electron microscopic data, the average size of polyhedral $Ag_xSC_{12}H_{25}$ nanoparticles was ~6.2 nm. Under short-term irradiation, the nanoparticles first decomposed to smaller particles (< 2 nm). However, an increase in the irradiation time to 9 min resulted in the appearance of larger (20-nm) particles. Photochemical transformations were detected from the time variations of the intensity and broadness of silver plasmon absorption lines (marked by heavy lines in Fig. 5). It was found that this absorption depends nonlinearly on the light intensity. The kinetics of photolysis of the particles was studied in the nanosecond range, and the corresponding kinetic constants were determined. Changes in the dielectric properties of the environment occurred within 0.5 ns. In response to optical excitation, a part of alkanethiol molecules were split off over the time (3.6 ns) determined by the energy liberated as heat (E_{th}). The proportion of particles with split off thiol groups depended on the excitation-pulse energy. Within 40 ns (recombination time), the thiol-covered particles could also undergo fragmentation. Subsequent exposure to light partially prevented fragmentation of nanoparticles.

In contrast to silver-based nanoparticles, which undergo light-induced chemical transformations, the behaviour of gold-based nanoparticles under similar conditions is characterised by changes in their shapes. Fragmentation of these nanoparticles is dramatically weakened both in polar solvents and with the changes in the length of the alkanethiol chain.[108]

Silver nanoparticles were used for carrying out photochemical transformations of phenazine and acridine.[109] Being adsorbed on the surfaces of silver particles, both molecules were found to decompose under the action of light in a single-photon process with N–C bond cleavage. The reaction rate and the degree of photodecomposition depended on the light wavelength. Being exposed to short-wave laser light, phenazine decomposed with the formation of graphite. The decomposition rate of phenazine was higher compared to acridine, which apparently is due to different orientation of these molecules on the surfaces of silver particles. The reason for the decomposition these molecules undergo on the surfaces of silver nanoparticles remains unclear.[109] The spectra of acridine adsorbed on nanoparticle surfaces revealed two new

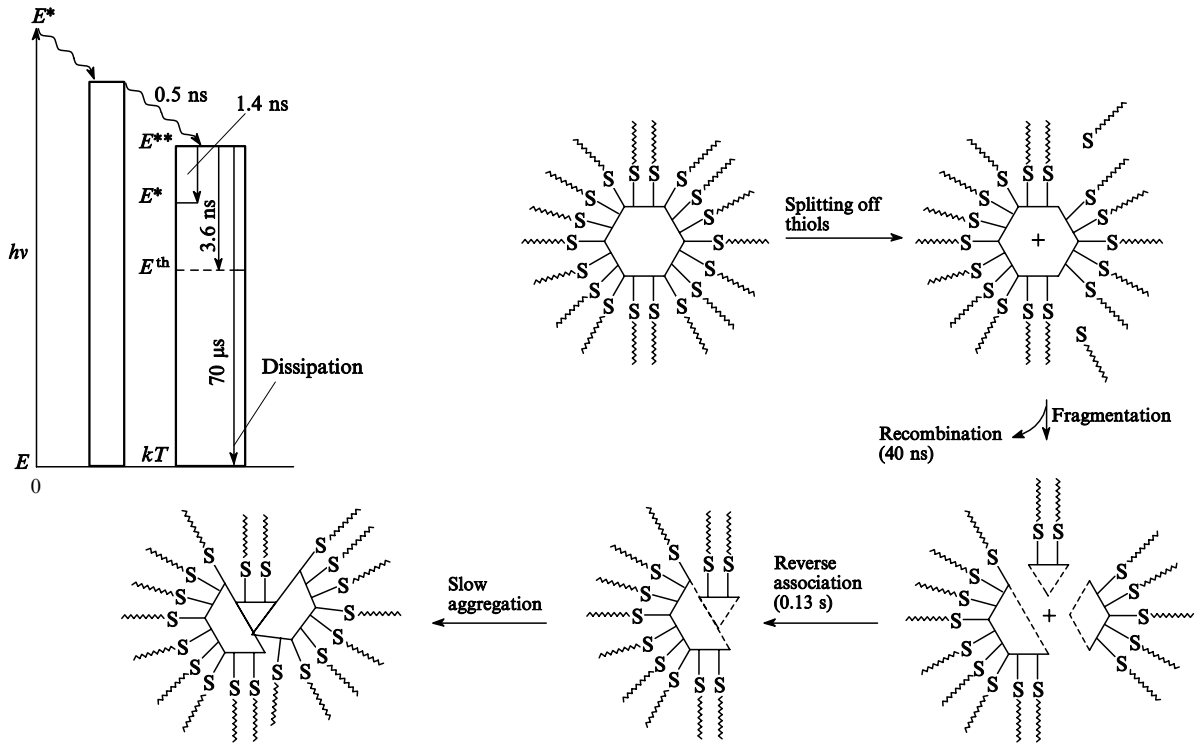


Figure 5. Schematic illustration of the photoreaction involving $Ag_xSC_{12}H_{25}$ dispersed in cyclohexane.[107]

bands at 543 and 619 cm^{-1}, which are close to those observed for quinazoline adsorbed on a silver surface.[110] It was noted that the rate and the extent of photoreactions described are not interrelated. It was assumed that to be decomposed the molecules of phenazine and acridine should either be adsorbed on certain surface sites or form definite geometrical configurations; hence, only a small proportion of molecules can be involved in the reaction.

Optical properties of gold nanoparticles with radii of 2.5, 9 and 15 nm prepared by γ-radiolysis of an aqueous solution of $KAuCl_4$ and stabilised in polyvinyl alcohol were studied.[111] It was found that solutions containing 2.5-nm particles do not attenuate transmitting light, whereas those with larger particles severely decrease the intensity of a laser pulse with a wavelength of 530 nm. The effects observed were attributed to the appearance of a great number of light-diffusion centres formed as a result of evaporation of gold nanoparticles under the laser pulse. Light-diffusion centres were formed in several nanoseconds and largely relaxed to the initial state; upon the next pulse, they partially degraded to small particles.

By means of time-resolved laser measurements, the electron–phonon interactions in metal particles based on Au particles with sizes ranging from 2 to 120 nm and in bimetallic particles based on Au, Ag and Pb were studied. Particles with Au cores and Ag shells and those with Au cores and Pb shells were studied in most details. All the particles were synthesised by radiolysis.[61] It was shown that for Au, in contrast, *e.g.*, to Ag, the time scale of the electron–phonon interaction is independent of the particle size.[112]

Finally, the studies dealing with the prospects of obtaining nanosize quantum dots, quantum wells and quantum wires in inorganic semiconductors [113] should be mentioned, as well as the works on nanophotonics. The latter studies optical properties of objects with much smaller sizes compared with the irradiation wavelength. The efforts were largely focused on investigation of linear optical effects, while the field of non-linear nanoscale optical phenomena is still under way.[114] The problems and prospects of nanophotonics were analysed in Ref. 115.

VI. Semiconductors and sensors

Semiconducting nanoparticles are widely used in heterogeneous catalysis, they are also promising materials for laser engineering, in manufacturing flat displays, light-emitting diodes and sensors. The use of AOT-based reverse micelles for the preparation of ZnSe nanoparticles was first reported in Ref. 116. ZnSe particles measuring 5.7 nm were studied using X-ray diffraction, electronic spectroscopy, light scattering, electron microscopy and luminescence techniques.

A method of stabilisation of nanoparticles of a semiconductor (exemplified by CdS, co-deposition of CdS–ZnS) and a metal (exemplified by gold) was put forward by Japanese scientists.[117] Reverse micelles were prepared and nanoparticles were stabilised by *in situ* polymerisation of (cetyl)dimethyl(*p*-vinylbenzyl)ammonium chloride which was initiated either by light or the addition of azobisisobutyronitrile. The polymer obtained was soluble in polar solvents and formed transparent films with incorporated nanoparticles of cadmium sulfide measuring from 4.7 to 6.3 nm. The proposed method seems to be versatile.

Internal cores of vesicles based on α-phosphatidylcholine can be used as 'nanoreactors' for growing monodispersed (with ~8% deviation) nanocrystals of CaS, ZnS, HgS with definite sizes.[118]

A simple and inexpensive method of synthesising gram quantities of stable water-soluble nanocrystalline powders of zinc sulfide (particles measuring ~6 nm) was put forward.[119] Cysteine-covered ZnS particles were obtained by introduction of sulfide to predissolved zinc salt and cysteine. Following deposition, redissolution and drying, crystalline ZnS powders were obtained, which remained stable for 30 months at 4 °C. Their stability was checked by carrying out catalytic decomposition of *p*-nitrophenol on freshly prepared and aged powders. Upon long-term storage, the optical properties of powders remained unchanged. Highly concentrated aqueous solutions (up to ~100 mmol $litre^{-1}$) of semiconducting particles were used as fluorescent biological labels.

Multilayer films incorporating CdSe nanoparticles were synthesised.[120] The particles measuring 1.7–2.0 nm were obtained from a dimethylformamide solution of cadmium salts and selenium. The films incorporating CdSe particles were prepared by successive formation of layers on quartz or CaF_2 plates. Layers of benzoic acid derivatives and polyvinylpyridine were first applied to the plate surface. The plate thus treated was placed in a dimethylformamide solution of CdSe in order to form a layer containing particles of cadmium selenide. Multilayer (up to five layers) films were obtained by severally adding polyvinylpyridine and cadmium selenide to the solution. Such films are interesting for the development of new types of light-emitting diodes and non-linear optical devices and can serve as conducting films.

Preparation of semiconducting nanowires of definite diameters by using colloidal nanoparticles of metal-catalysts was described.[121–124] As an example, we consider the results of controlled synthesis of GaP nanowires with diameters of 10, 20 and 30 nm and lengths exceeding 10 μm.[124] The wires were obtained by laser ablation of a solid target made of GaP and gold (catalyst). For this purpose, a solution that contained gold particles was applied on a target. The latter was placed in a quartz tube with a solid ZnS target. The tube was located in a blown end of an oven, which was heated to 700 °C and the target was ablated for 10 min by means of an excimer laser. Simultaneous generation of nanoclusters of gold and of GaP semiconductor occurred; the latter particles formed semiconducting nanowires.

Control experiments have shown that in the absence of gold particles no semiconducting wires form. A relationship between the sizes of gold nanoparticles and the diameters of semiconducting GaP wires allowed the authors to conclude that the diameters of the wires obtained can be controlled. A similar method of governing the diameters of silicon nanowires was proposed.[123]

The effect of the size of a semiconducting nanoparticle on its forbidden gap width was studied using CdSe particles measuring from 0.7 to 2 nm as an example.[125,126] All the particles were obtained by using the methods of organometallic chemistry so that their surfaces bore phosphorus atoms and phenyl and propyl groups. For example, the composition of one of the particles studied was $Cd_{10}Se_4(SePh)_{12}(PPr_3)_4$. The atomic structure of the particles was determined using the X-ray diffraction technique. Figure 6 shows the dependence of the forbidden gap width of cadmium selenide nanoparticles on their sizes. It is seen that as the

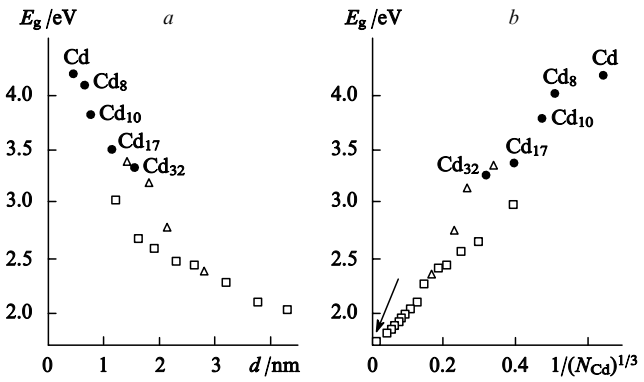


Figure 6. Forbidden gap thickness of CdSe nanoparticles as a function of their (*a*) diameter and (*b*) reciprocal radius.[125] *N* is the number of atoms in a particle. Black points are experimental data, open points are literature data for larger particles (results by different authors). The arrow marks a bulk particle.

nanoparticle size increases the forbidden gap width (E_g) of a particle approaches the E_g value of CdSe bulk samples.

Dynamic properties of charge carriers on the liquid–semiconductor interface are important for photocatalysis, solar energy conversion and photoelectrochemistry. The properties of charge carriers, *viz*., electrons and holes, were studied in a number of semiconducting nanosystems using laser techniques.[127]

Suspensions of cadmium sulfide nanoparticles were used for the initiation of acrylonitrile polymerisation. The polyacrylonitrile (PAN) obtained and the products of its partial hydrolysis were used as the templates which governed the shapes of CdS nanoparticles and CdS/PAN composite nanowires with diameters of 6 nm and lengths varying from 200 nm to 1 μm.[128]

A nanosize electronic switch was built of gold nanoclusters and compounds containing redox groups.[129] Synthesis of *N,N′*-di(10-mercaptodecyl)-4,4′-bipyridinium dibromide containing a bipyridinium fragment as the redox group was described.[130] When gold nanoparticles are bound to the film of bipyridinium dibromide molecules, the reduction of the bipyridinium group on a gold electrode proceeds readily and reversibly.

$$bipy^{2+} + e^- \rightleftharpoons bipy^{+\bullet}.$$

Figure 7 schematically shows an electronic switch measuring less than 10 nm which is controlled by the voltage applied to the STM probe.§ When a molecule involves bipyridinium in a reduced ($bipy^{+\bullet}$) state, a noticeable tunnelling current flows in the nanocluster–molecule–electrode circuit. If a certain threshold voltage is applied to the gold electrode, the tunnelling current decreases. The threshold voltage corresponds to the oxidation of $bipy^{+\bullet}$ to $bipy^{2+}$. At present, such devices operate slowly and require an amplifier. However, they can be used in those fields where amplification is of less importance, *e.g*., as the chemical sensors for detection of single molecules or individual chemical reactions. Moreover, based on these systems, memory devices for computers can be developed.[131]

§ The scheme is taken from Ref. 131, in which the results of another study (Ref. 130) are commented upon. The system shown was assumed [130] to correspond to approximately 60 organic molecules and required no less than 30 electrons to operate.

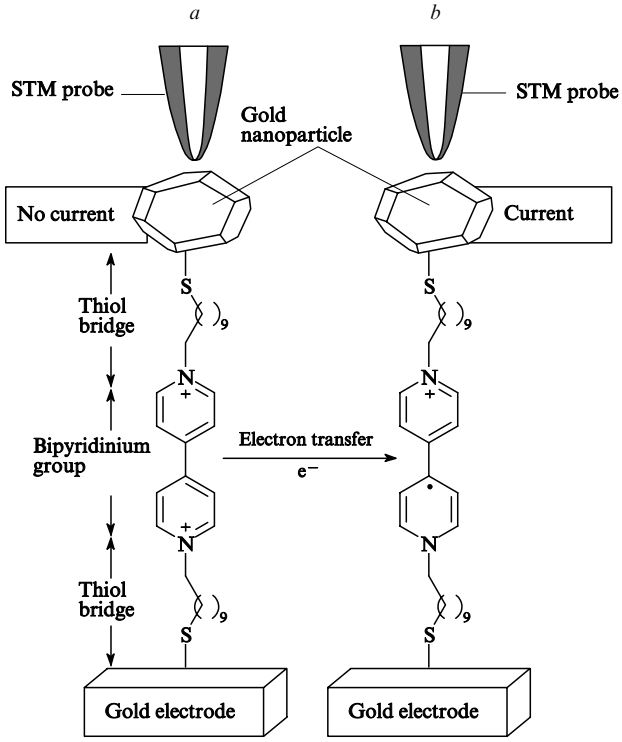


Figure 7. Schematic illustration of the performance of an electronic switch.[131] (*a*) Bipyridinium group is in the oxidised state and no current flows, (*b*) accepting an electron, the bipyridinium group is reduced and a current arises.

New possibilities in designing sensors and optoelectronic devices including those with nanoparticles have been pioneered.[132] It was shown that pore-free crystals of organoplatinum compounds can reversibly absorb and evolve sulfur dioxide without any losses in their crystallinity. Figuratively speaking, the crystals 'breath'. Figure 8 schematically shows the corresponding transitions.

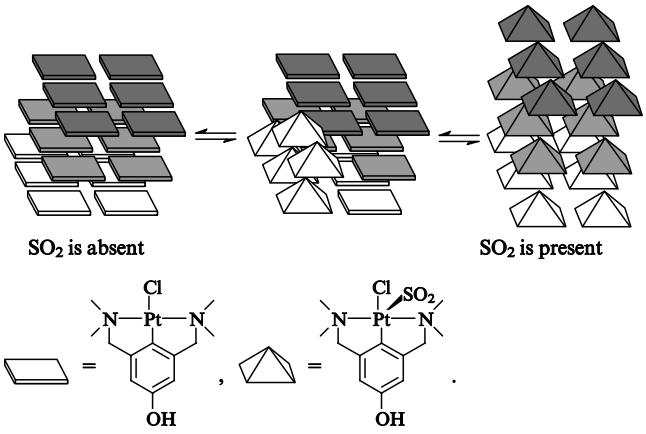


Figure 8. Crystals that reversibly absorb SO_2.[133]

On being exposed to SO_2 for one minute, the crystal acquires an orange colouring. The colour change is accompanied by a transition of planar square platinum complexes into square-pyramidal complexes which involve SO_2 as the fifth ligand. In the process, the crystal increases its volume by 25% but retains the ordered crystal structure. Then, if the crystal is exposed to air, it breathes out SO_2 and relaxes to its initial colourless SO_2-free state. The process can be repeated many times without loss of the crystallinity. It was suggested to use such crystals as optical switches and SO_2-sensors. It is possible that some other similar compounds can reversibly interact with chlorine, CO_2 and other gases. There are strong grounds to believe that substances that bind gases in solution can also bind them in the solid state.

Nanocrystalline films of semiconducting oxides can also be used as the sensitive units of gas sensors. The effects of ethanol and nitrogen dioxide vapours on the properties of SnO_2 nanocrystals applied on single-crystal silicon and of SnO_2 nanocrystals doped by nickel, palladium and copper were studied.[134] Doped SnO_2 nanocrystals were synthesised by pyrolysis of aerosols. According to X-ray diffraction data, their average size was 6–8 nm. It was shown that diffusion of gases affects the voltammetric characteristics of heretostructures, which manifests itself in variations of the potential-barrier height on the heterogeneous boundary and in the changes in the tunnelling processes at the interface.

A new generation of chemical sensors can be synthesised by using non-uniform nanosystems and unusual electronic and physicochemical properties of nanoparticles involved in such systems. In these systems, compact crystalline cores of nanoparticles are surrounded by outer amorphous shells, and the electron transfer induced by adsorbed gas molecules proceeds through the nanoparticles arranged in ensembles and interacting with one another. The sensor properties of non-uniform nanocomposite films were studied[135] for the oxide–oxide (SnO_2–TiO_2), metal–oxide (Cu–SiO_2) and metal–polymer [Cu–poly(*p*-xylylene)] systems. The sensor activities of the specimens with respect to hydrogen, wet air and ammonia were

determined from conductivity variations. All specimens were synthesised under non-equilibrium conditions, which seems to be necessary for the preparation of effective sensor materials.

VII. Catalysis on nanoparticles

The studies devoted to using nanoparticles in the development of novel catalysts which were published before 2000 are surveyed in detail by Bukhtiyarov and Slin'ko.[14] In this section, we consider only the studies published in 2000.

Methane combustion in air proceeds steadily at temperatures above 1300 °C. However, at these temperatures, noxious nitrogen oxides evolve resulting in smog. In this connection, the search for new catalysts of methane combustion is urgent. A new catalyst was synthesised[136] which provided methane combustion at 400 °C. This was prepared using reverse microemulsions based on isooctane, water and surfactants such as the polyethylene oxide–alcohol adducts. Alkoxides $Ba(OC_3H_7)_2$ and $Al(OC_3H_7)_3$ were dissolved in isooctane and mixed with the microemulsion at room temperature: the resulting solid crystalline nanosize barium hexaaluminate exhibited high catalytic activity in CH_4 combustion. The advantage of barium hexaaluminate lies in the fact that the sizes and surfaces of its particles remain unchanged at high temperatures. Moreover, this can be modified by cerium, cobalt, manganese and lanthanum. Modification with cerium oxide produced a composite which enabled methane combustion at temperatures below 400 °C. The history of the search for new methane-combustion catalysts and their characteristics are described elsewhere.[137]

In aqueous AOT–n-heptane buffer microemulsions, a number of reactions were catalysed by palladium nanoparticles. The reaction of *N,N*-dimethyl-*p*-phenylenediamine with $Co(NH_3)_5Cl^{2+}$ catalysed by palladium nanoparticles was described.[138] The catalytic oxidation of *N,N,N′,N′*-tetramethyl-*p*-phenylenediamine by $Co(NH_3)Cl^{2+}$ was also studied in similar microemulsions at pH 5.6.[139] The limiting stage of the reaction was the adsorption of *p*-phenylenediamine on palladium particles of 2.5-nm radii within the microemulsion. This conclusion relies on an observation that the activation energy of the reaction changes from 97 at 15 °C to 39 kJ mol^{-1} at 40 °C and on the results of electrochemical measurements. The specific features of the reaction were discussed in terms of the microreactor model.

Synthesis of platinum, palladium, rhodium and iridium nanoparticles and their use in catalytic hydrogenation of cyclooctene, dodec-1-ene and *o*-chloronitrobenzene were described.[140] Nanoparticles were synthesised by reduction of metal salts by alcohols and stabilised by an amphiphilic copolymer of 1-vinylpyrrolidone with acrylic acid (PVP–AA). The diameters of particles were 0.74 (Ir), 1.93 (Rh), 2.2 (Pd) and 1.2–2.2 nm (Pt), which were determined by electron microscopy.

The introduction of nickel ions into the PVP–AA–Pt catalytic system enhances the effeciency of the latter. Hydrogenation of chloronitrobenzene to chloroaniline at 330 K was carried out with a selectivity of 97.1% and 100% conversion. Introduction of Co^{2+} and Fe^{3+} ions reduced the hydrogenation selectivity to 78.1% and 72.1%, respectively. The analysis of IR spectra have shown that, on being exposed to hydrogen, the ions of nickel, iron and cobalt were not reduced to zero-valent metals. This was explained by the fact that the metal ions interact with two C=O groups in the PVP–AA copolymer and only with a single C=O group in poly(1-vinylpyrrolidone).[141]

The problems of measuring sizes of metal particles applied on supports and size and surface-area distributions for particles with diameters smaller than 2.5 nm were discussed in Ref. 142.

When chemisorption is used for the determination of a catalyst's properties, it is necessary to know how to follow catalyst operation with contaminated surfaces and make an allowance for strong interaction of the metal with the support. A systematic study (in the temperature interval of 573–973 K) of palladium particles of average size ~2 nm applied on activated carbon has been accomplished.[143] The use of two methods, *viz*., X-ray small-angle scattering and transmission electron microscopy allowed the effective sizes of palladium particles to be estimated and the results to be compared with the data obtained in studying CO chemisorption on supported palladium. The agreement between the results of two aforementioned methods was observed for the stoichiometric ratio Pd : CO = 2.

A high catalytic activity of nanoparticles composed of metal cores and outer shells was demonstrated in several studies.[144–147] Gold nanoparticles measuring 2 and 5 nm surrounded by decanethiol molecules were used for electrochemical oxidation of carbon monoxide.[145] Figure 9 schematically shows the electrode reaction. It is noteworthy that the use of thiol-covered gold nanoparticles suggests a co-operative increase in the catalytic activity.

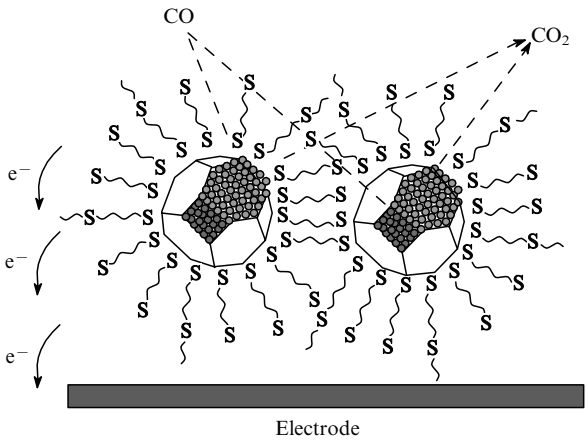


Figure 9. Catalytic oxidation of carbon monoxide on an ensemble of thiol-covered gold nanoparticles on the electrode surface.

The methods of preparation of optimal catalysts may involve varying the shapes of cores, the structures and properties of molecular shells and the types of core–shell bonding. The latter factor affects active sites, defect packing and co-operative electronic properties of nanoparticles.

Platinum nanoparticles were obtained by reducing chloroplatinic acid ($H_2PtCl_6 \cdot 6H_2O$) by ethanol in the presence of poly(*N*-vinylformamide), poly(*N*-vinylacetamide), poly(*N*-isopropylacrylamide) or poly(*N*-vinylpyrrolidone). The particles synthesised had an average diameter of ~2.0–2.5 nm.[148] The effects of additon of KCl and Na_2SO_4 and of temperature variations on the stability of nanoparticles were studied. The particles obtained were used in hydrogenation of allyl alcohol in water and in a salt solution (0.8 M Na_2SO_4). It was shown that catalytic platinum particles are stable in the salt solution and their activity is equal to that in water.

Bimetallic Au–Pt/C(graphite) catalysts were prepared by selective deposition of gold on a platinum film on graphite as a support.[149] The latter monometallic catalyst was obtained by the reduction of H_2PtCl_6 in anhydrous ethanol. The monometallic catalyst was modified by two methods. The first method used platinum as the reagent which reduced $AuCl_4^-$. In the other method, the monodispersed catalyst was first treated with hydrogen and then $HAuCl_4$ was added. At pH 1, bimetallic particles were formed according to the reaction

$$3\,PtH + AuCl_4^- \longrightarrow Pt_3Au + 4\,Cl^- + 3\,H^+.$$

The average size of particles was ~10 nm. The properties of particles and their reactions were studied by several techniques.

Being chemically inactive, gold did not attract much attention as a catalyst until recently. However, gold ions Au^{n+} ($1 \leqslant n \leqslant 3$) in zeolites turned out to be active in the reaction

$$H_2O + CO \longrightarrow H_2 + CO_2$$

at 323 K.[150]

Lithographic systems comprising SiO_2-supported platinum nanoparticles and Al_2O_3-supported silver nanoparticles, which were prepared using electronic beams, were used as model metallic catalysts.[151] The particles with the average sizes of 20–50 nm were spaced at 100–200 nm. The thermal stability of the systems obtained was studied by means of electron microscopy and AFM. The system with platinum particles was stable up to 973 K, whereas the system with silver particles was stable up to 773 K in both vacuum and hydrogen and up to 623 K in oxygen. The catalytic effect of a model catalyst with SiO_2-supported platinum nanoparticles was compared to that of a platinum foil in hydrogenation and dehydrogenation of cyclohexene at 100 °C.[152] The reactivity of a system with platinum particles of 28 nm diameter was shown to be twice as high compared with that of the foil, and its selectivity was higher by a factor of 3.

Isomerisation of dichlorobutanes catalysed by iron-containing nanoparticles stabilised in polymeric matrices was studied.[153] The catalytic activity was shown to depend on the nature of the matrix and the metal content.

Photocatalytic reduction of bis(2-bipyridyl) disulfide (RSSR) to pyridine-2-thiol (RSH) by water selectively proceeded on the surface of titanium dioxide. The reaction rate substantially increased when silver nanoparticles (0.24 mass %) with sizes < 1 nm were applied on TiO_2.[154]

The following mechanism was assumed [154] for this reaction:

$$(1)\ RSSR + 2\,AgTiO_2 \overset{K_a}{\rightleftharpoons} 2\,RSAgTiO_2,$$

$$(2)\ 2\,RSAgTiO_2 \xrightarrow{I\varphi} 2\,RSAgTiO_2(e^- \ldots h^+),$$

$$(3)\ 2\,RSAgTiO_2\,(e^- \ldots h^+) \xrightarrow{k_{d1}} 2\,RSAgTiO_2,$$

$$(4)\ 2\,RSAgTiO_2\,(e^- \ldots h^+) \xrightarrow{k_{cs}} 2\,RSAg(e^-)TiO_2(h^+),$$

$$(5)\ 2\,RSAg(e^-)TiO_2(h^+) \xrightarrow{k_{d2}} 2\,RSAgTiO_2,$$

$$(6)\ 2\,RSAg(e^-)TiO_2(h^+) + H_2O \xrightarrow{k_0} 2\,RSAg(e^-)TiO_2 + 2\,H^+ + \frac{1}{2}O_2,$$

$$(7)\ 2\,RSAg(e^-)TiO_2 + 2H^+ \xrightarrow{k_r} 2\,RSH + AgTiO_2,$$

where K_a is the equilibrium adsorption constant, I is the light intensity, φ is the intensity of light absorption.

In the first stage, the selective adsorption of RSSR on the surfaces of silver nanoparticles is accompanied by the cleavage of the S–S bond. In the second stage, upon the excitation of nanoparticles in the forbidden gap range of TiO_2, an electron (e^-)–hole(h^+) pair is generated. Most of electron–hole pairs recombine (stages *3* and *5*). In stage *4*, charge separation occurs: silver nanoparticles accept electrons, and holes are transferred to the TiO_2 support. The positive potential of a hole is sufficient for water to be oxidised with the formation of H^+ ion and O_2 molecule (stage *6*). In stage *7*, the catalytic system is reduced producing RSH. As a result, the deposited silver nanoparticles seem [154] to cause the following effects:

— acceleration of RSSR adsorption;

— space separation of sites responsible for reduction (silver particles) and oxidation (TiO_2 support), *i.e.*, the effect of charge separation;

— selective adsorption of the substance to be oxidised (RSSR) and the reducing agent (H_2O) in the reduction and oxidation sites, which makes the process highly selective.

Comparison of TiO_2 and $AgTiO_2$ catalytic systems has shown that both systems provide equal activation energies in the photocatalytic reduction (30 ± 1.5 kJ mol^{-1}), which suggests that the multistage process is limited by stage *6* rather than by photocatalysis. Below, the reduction on TiO_2 is shown.

$$2\,RS...TiO_2(e^-) + 2\,H^+ \xrightarrow{k_r} 2\,RSH + TiO_2.$$

In recent years, semiconducting nanoparticles have been actively used in photocatalysis. In this connection, the catalytic activities of nanoparticles of different oxides and sulfides in aqueous and polar (acetonitrile) organic solvents were compared [155] using photooxidation of pentachlorophenol (a toxic compound used as a fungicide and a bactericide and for wood conservation) as an example. Figure 10 shows the relative concentration of pentachlorophenol as a function of the time of its exposure to light in the presence of nanoparticles of different metal sulfides.

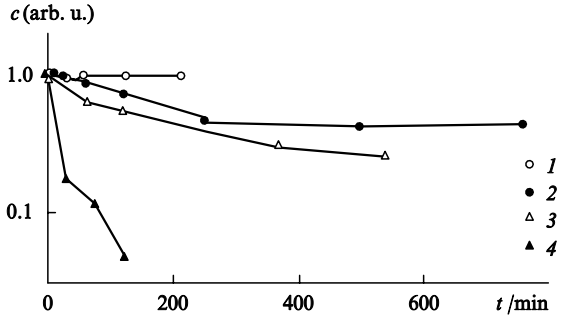


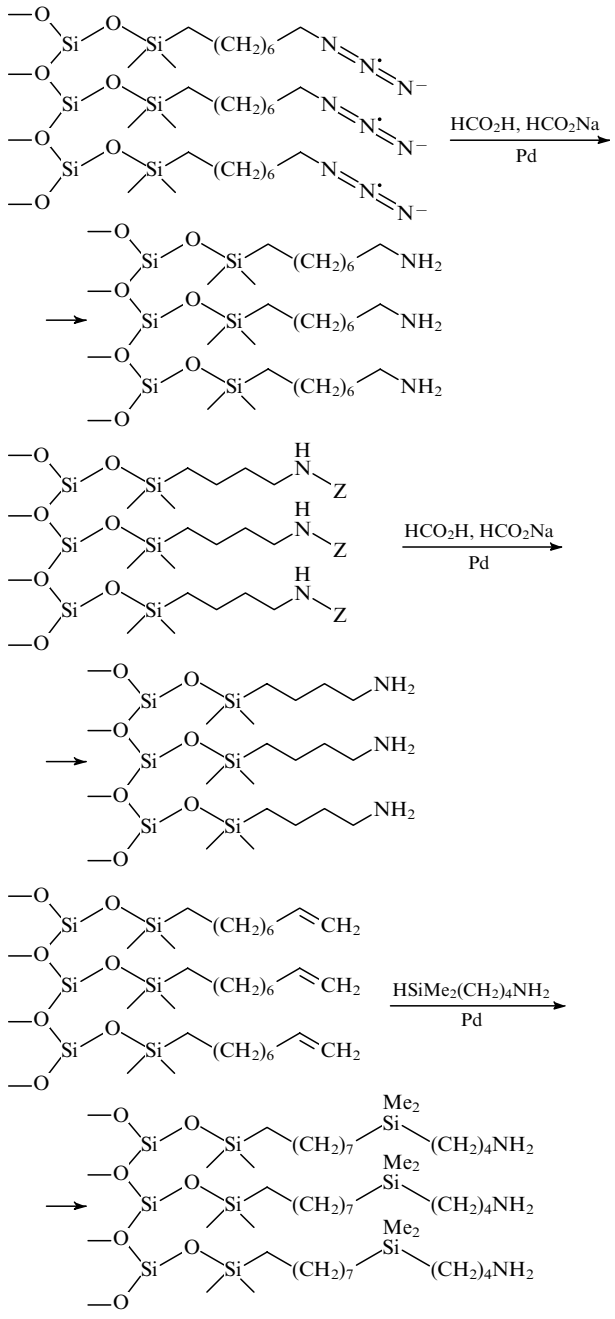
Figure 10. Changes in the relative concentration of pentachlorophenol (c) in water with the time of its exposure to light of the wavelength $400 < \lambda < 700$ nm (*1*) in the absence and (*2–4*) in the presence of catalysts.[155] (*1*) Without catalyst (or TiO_2); (*2*) CdS powder (0.1 mg ml^{-1}), (*3*) MoS_2 particles with diameters of 4.5 nm (0.036 mg ml^{-1}), (*4*) MoS_2 particles with diameters of 3 nm (0.09 mg ml^{-1}).

It is of note that the effect of the nanoparticle size on the reaction rate is extremely strong for MoS_2 particles. This reflects the effect of the forbidden gap width of particles on the reaction and is associated with the corresponding change in the reduction potential. In contrast to a common photocatalyst, *viz.*, titanium oxide, which is active in the UV region, molybdenum disulfide particles measuring 3 nm catalyse the reaction in the visible range. When SnO_2 nanoparticles measuring 26 and 58 nm were used, the nanoparticle size did not significantly affect the photooxidation of pentachlorophenol.

One can predict the development of a new direction of nanochemistry which is associated with realisation of chemical reactions by means of AFM and STM probes. Interesting examples of chemical modification of terminal functional groups in aggregates of organosilicon molecules were carried out by the catalytic action of an AFM probe covered (at open circuit conditions) with palladium.[156]

A minimum effort required for such chemical reactions to occur is ~2.5 μN at a scanning rate below 5 μm s^{-1}. It should be noted that the typical activation energy of the bimolecular reactions shown is ~50 kJ mol^{-1}. At the same time, according to estimates, the energy of surface deformation of an associate formed by organosilicon molecules is ~340 kJ mol^{-1}, which far exceeds the activation energy.

An approach to 'chemical lithography', which consists in chemical modification of functional groups in the molecules arranged along definite preset lines in a sample, was first documented in Ref. 157.



Z is a benzyloxycarbonyl group.

VIII. Nanoparticles in biology and medicine

At present, a new direction of nanochemistry is being developed vigorously. The goal of these studies is the synthesis and application of systems comprising metal nanoparticles (mainly, gold and silver) and various biomolecules: DNA, peptides and oligonucleotides. The optical properties of aggregates of gold nanoparticles bound by DNA fragments containing from 27 to 72 nucleotide pairs were discussed.[158] Alkanethiol-modified gold particles of diameter $\sim$15 nm were used. The effect of the length of an oligonucleotide chain on the optical properties of aggregates obtained was studied, and the position of the metal plasmon peak was found to depend on the chain length. The sizes of nanoparticle aggregates were determined by the kinetic method, because their growth rate depended on the lengths of oligonucleotide chains and on the distances between nanoparticles. Among the factors that affect the growth rate of aggregates, the rate of binding of DNA linkers ¶ with complementary DNA molecules on the surfaces of gold nanoparticles (k_1) and the rate of aggregate growth (k_2) are the most important. Optical changes were also observed upon annealing of structures formed by two longest nucleotides-linkers at temperatures below their melting point. Thus, DNA linkers can be used for kinetic control over aggregate growth.

A new method of introduction of biomaterials into living cells was proposed [159] based on electrospraying of metal particles with large electrical charges and high velocities. If one disperses gene-covered metal particles using the equipment developed, these particles disintegrate in liquid drops under the external non-uniform field. Gene fragments thus obtained have charges of the same sign as the metal particles and are present in high concentrations. Monkey fibroblasts were used as the living cells and either suspensions of plasmids † labelled with fluorescent peptides or plasmids with gold nanoparticles measuring 5–10 nm were used as the biomaterials. UV fluorescent microscopic studies have shown plasmid suspensions with gold particles to penetrate into cells. The fact that gold-free plasmid suspensions also penetrated into the cells and got incorporated into its DNA is of prime importance. This result seems to be most significant, because this allows one to dispense with gold traditionally used for these purposes. It was noted that electrostatic spraying opens up new possibilities for transfection of genes and gene therapy.

Nanoparticles doped with gadolinium ions were proposed for use as new contrast materials for NMR studies in medicine. Such nanoparticles with diameters of 120 nm are sufficiently small to penetrate easily into blood vessels. These have been used for obtaining the images of hearts and gastric channels in rats.[160]

Approaches to using biomolecules for identification of common inorganic materials are being developed. These can be realised by applying the principles of selective binding known from molecular biology. Selective binding of peptides to different semiconductors was proposed as a method of preparation of nanocrystalline ensembles.[161] It was shown that nanocrystalline semiconductors can be used for the isolation of certain peptides which bind specifically to the semiconductor surface. Five different faces of semiconducting single crystals were used, as the substrates, *viz*., GaAs(100), GaAs(111)Ga (with Ga atoms on the surface), GaAs(111)As (with As atoms on the surface), InP(100) and Si(100). Each substrate was found to select and bind certain amino acid sequences from a large number of random peptides. The nanocrystalline ensembles obtained were studied using antibodies labelled with 20-nm gold nanoparticles and the methods of transmission and fluorescent microscopy, photoelectron spectroscopy and atomic-force and scanning tunnelling microscopy.

Figure 11 illustrates two different approaches to the development of biomolecular ensembles on surfaces of inorganic materials.[162] Development of these approaches is a challenge to materials science of the XXIst century.

In this context, attention should be drawn to a study [163] in which the prospects of synthesising two- and three-dimensional nanostructures based on biological principles were considered. It is believed that the strategy of synthesising complex ensembles from simpler ones will be developed in the new century. Biological structures may be used as surface detectors which organise binding of large organic and inorganic building blocks. Indeed, in this approach, the principles developed in the course of evolution for building new functional structures may be used for synthesising new materials.

¶ Linkers are nonhelical segments of a double-stranded DNA which interlink compact DNA segments stabilised by peptides and polyamines.
† Plasmids are extrachromosome formations representing closed circles of double-stranded DNA.

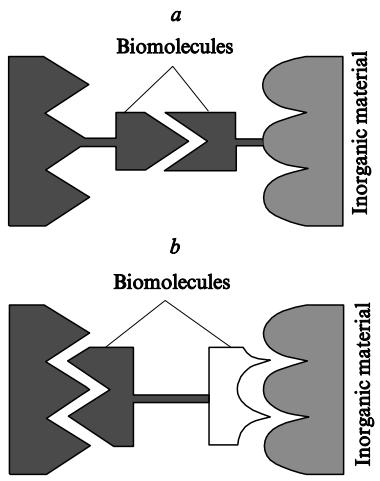


Figure 11. Two approaches to assembly of inorganic materials into complex structures with the use of biological molecules.
(*a*) The use of complementarity of two biomolecules, (*b*) the use of biomolecule interaction with an inorganic material.[162]

IX. Conclusion

The analysis of studies published in recent years shows that many aspects of nanochemistry of metals and semiconductors are gaining importance, and considerable progress has been made towards their solution.

The factors that affect the sizes and shapes of nanoparticles during their synthesis, the processes of self-assembly of both nanoparticles themselves and ligands that stabilise them are being actively studied. The list of polymers, surfactants, reversed micelles and thiols, which are traditionally used for the stabilisation of nanoparticles, was successfully replenished with dendrimers. The use of nanoparticles in catalysis has been extended, as well as the use of semiconducting particles in photocatalysis. The studies in which metal nanoparticles are used in carrying out unusual reactions are conducted more intensively. The problem of synthesising and studying the reactions of non-protected metal nanoparticles becomes increasingly pressing. Interest is shifting to reactions of metal nanoparticles measuring less than 1 nm. In this aspect, the use of inert gas at low and superlow temperatures as the matrices for the synthesis of nanoparticles seems to be very promising.

Yet another challenging direction of nanochemistry may be developed at the boundary of such sciences as biology, organic and inorganic chemistry and materials science. Mutual 'recognition' and joint self-assembly of inorganic and biological molecules are the key problems which being solved, will provide new advanced materials.[164]

At the beginning of 2000, a new programme aimed at the development of fundamental and applied studies in nanotechnology was formulated in the USA.[165] In 2001, this issue is additionally financed by 500 million dollars. The following directions were chosen as the most challenging:

— the use of modern experimental equipment for studying the processes which involve nanoparticles or proceed on the surfaces of nanostructures;

— elucidation of the roles nanoparticles play in such important processes as deposition of proteins, desorption of contaminants, stabilisation of colloidal dispersions, aggregation of micelles and control over microorganism mobility;

— development of experimental techniques and their computerisation for studying the role of nanoparticles in the processes that occur in the atmosphere and water sources;

— the use of mesoporous structures integrated with appropriate microcomponents to provide highly sensitive and highly selective contamination detectors.

In conclusion, it should be stated that at present the studies of nanoparticle properties form an interdisciplinary scientific field which largely determines the development of the other neighbouring fields.

The author is grateful to his co-workers, post-graduate students and students of the Laboratory of Low-Temperature Chemistry for their assistance in the preparation of this review. This review was partially financially supported by the Russian Foundation of Basic Research (Project No. 99-03-32206).

References

1. K J Klabunde *Free Atoms, Clusters and Nanoscale Particles* (San Diego; New York; Boston; London; Sydnay; Tokyo: Academic Press, 1994)
2. G B Sergeev, in *Khimicheskaya Fizika na Poroge XXI v* (Chemical Physics at the Threshold of the XXIst Century) (Moscow: Nauka, 1996) p. 149
3. G B Sergeev, M A Petrukhina *Prog. Solid State Chem.* **24** 183 (1996)
4. A D Pomogailo *Usp. Khim.* **66** 750 (1997) [*Russ. Chem. Rev.* **66** 679 (1997)]
5. R F Khairutdinov *Usp. Khim.* **67** 125 (1998) [*Russ. Chem. Rev.* **67** 109 (1998)]
6. A S Edelstein, R C Cammarata (Eds) *Nanomaterials: Synthesis, Properties and Applications* (Bristol: J N Arrowsmith Ltd, 1998)
7. J H Fendler (Ed.) *Nanoparticles and Nanostructured Films* (New York: Wiley-VCH, 1998)
8. B G Ershov *Izv. Acad. Nauk, Ser. Khim.* 1 (1999) [a]
9. G B Sergeev *Vestn. Mosk. Univ., Ser. 2, Khim.* **40** 312 (1999) [b]
10. A D Pomogailo, A S Rozenberg, I E Uflyand *Nanochastitsy Metallov v Polimerakh* (Metal Nanoparticles in Polymers) (Moscow: Khimiya, 2000)
11. H Gleiter *Acta Mater.* **48** 1 (2000)
12. B D Summ, N I Ivanova *Usp. Khim.* **69** 995 (2000) [*Russ. Chem. Rev.* **69** 911 (2000)]
13. V I Roldughin *Usp. Khim.* **69** 899 (2000) [*Russ. Chem. Rev.* **69** 821 (2000)]
14. V I Bukhtiyarov, M G Slin'ko *Usp. Khim.* **70** 167 (2001) [*Russ. Chem. Rev.* **70** 147 (2001)]
15. I P Suzdalev, P I Suzdalev *Usp. Khim.* **70** 203 (2001) [*Russ. Chem. Rev.* **70** 177 (2001)]
16. A L Buchachenko *Usp. Khim.* **68** 99 (1999) [*Russ. Chem. Rev.* **68** 85 (1999)]
17. M A El-Sayed *J. Phys. Chem.* **95** 3898 (1991)
18. C S Feigerle, S Bililign, J C Miller *J. Nanopart. Res.* **2** 147 (2000)
19. T Yonezawa, S Onoue, N Kimizuka *Langmuir* **16** 5218 (2000)
20. L M Bronstein, D M Chernyshov, P M Valetsky, E A Wilder, R J Spontak *Langmuir* **16** 8221 (2000)
21. D I Svergun, E V Shtykova, M B Kozin, V V Volkov, A T Dembo, E V Shtykova Jr , L M Bronstein, O A Platonova, A N Yakunin, P M Valetsky, A R Khokhlov *J. Phys. Chem. B* **104** 5242 (2000)
22. B G Ershov, N L Sukhov, E Janata *J. Phys. Chem. B* **104** 6138 (2000)
23. B G Ershov *Izv. Akad. Nauk, Ser. Khim.* 1733 (2000) [a]
24. A Henglein *J. Phys. Chem. B* **104** 1206 (2000)
25. S Wang, H Xin *J. Phys. Chem. B* **104** 5681 (2000)
26. Z L Wang *J. Phys. Chem. B* **104** 1153 (2000)
27. L Rodrigues-Sanchez, M L Blanko, M A Lopez-Quintela *J. Phys. Chem. B* **104** 9683 (2000)
28. E E Foos, R M Stroud, A D Berry, A W Snow, J P Armistead *J. Am. Chem. Soc.* **122** 7114 (2000)
29. J Fang, K L Stokes, J Wiemann, W Zhou *Mater. Lett.* **42** 113 (2000)
30. L M Bronstein, D M Chernyshov, G I Timofeeva, L V Dubrovina, P M Valetsky, A R Khokhlov *J. Colloid Interface Sci.* **230** 140 (2000)
31. M-H Lee, S-G Oh, S-C Yi *J. Colloid Interface Sci.* **226** 65 (2000)
32. O E Litmanovich, A A Litmanovich, I M Papisov *Vysokomol. Soedin., Ser. A* **42** 670 (2000) [c]
33. S Keki, J Torok, G Deak, L Daroczi, M Zsuga *J. Colloid Interface Sci.* **229** 550 (2000)

34. F Grohn, B J Bauer, Y A Akpalu, C L Jackson, E J Amis *Macromolecules* **33** 6042 (2000)
35. K Esumi, T Hosoya, A Suzuki, K Torigoe *J. Colloid Interface Sci.* **226** 346 (2000)
36. M Liu, X Yan, H Liu, W Yu *React. Funct. Polym.* **44** 55 (2000)
37. H W Rollins, F Lin, J Johnson, J-J Ma, J-T Liu, M-H Tu, D D DesMarteau, Y-P Sun *Langmuir* **16** 8031 (2000)
38. O Siiman, A Burshteyn *J. Phys. Chem. B* **104** 9795 (2000)
39. J S Bradly, B Tesche, W Busser, M Maase, M T Reetz *J. Am. Chem. Soc.* **122** 4631 (2000)
40. M V Kiryukhin, B M Sergeev, A N Prusov, V G Sergeev *Vysokomol. Soedin., Ser. B* **42** 2171 (2000) [c]
41. M V Kiryukhin, B M Sergeev, A N Prusov, V G Sergeev *Vysokomol. Soedin., Ser. B* **42** 1069 (2000) [c]
42. A Miyazaki, Y Nakano *Langmuir* **16** 7109 (2000)
43. J Zhu, S Liu, O Palchik, Y Koltypin, A Gedanken *Langmuir* **16** 6396 (2000)
44. J Zhu, S T Aruna, Y Koltypin, A Gedanken *Chem. Mater.* **12** 143 (2000)
45. A A Mamedov, N A Kotov *Langmuir* **16** 5530 (2000)
46. S Sun, C B Murray, D Weller, L Folks, A Moser *Science* **287** 1989 (2000)
47. X Peng, L Manna, W Yang, J Wickham, E Scher, A Kadavanich, A P Alivisatos *Nature (London)* **404** 59 (2000)
48. S-J Park, S Kim, S Lee, Z G Khim, K Char, T Hyeon *J. Am. Chem. Soc.* **122** 8581 (2000)
49. M Sastry, A Gole, S R Sainkar *Langmuir* **16** 3553 (2000)
50. Z L Wang, R P Gao, B Nikoobakht, M A El-Sayed *J. Phys. Chem. B* **104** 5417 (2000)
51. A S Eppler, G Rupprechter, E A Anderson, G A Somorjai *J. Phys. Chem. B* **104** 7286 (2000)
52. C L Carnes, K J Klabunde *Langmuir* **16** 3764 (2000)
53. G W Wagner, O B Koper, E Lucas, S Decker, K J Klabunde *J. Phys. Chem. B* **104** 5118 (2000)
54. P Poisot, S Laruelle, S Gruqeon, L Dupont, J-M Tarascon *Nature (London)* **407** 496 (2000)
55. S H Elder, F M Cot, Y Su, S M Heald, A M Tyryshkin, M K Bowman, Y Gao, A G Joly, M L Balmer, A C Kolwaite, K A Magrini, D M Blake *J. Am. Chem. Soc.* **122** 5138 (2000)
56. J P Novak, D L Feldheim *J. Am. Chem. Soc.* **122** 3979 (2000)
57. A C Templeton, W P Wuelfing, R W Murray *Acc. Chem. Res.* **33** 27 (2000)
58. W P McConnell, J P Novak, L C Brousseau III, R R Fuierer, R C Tenent, D L Feldheim *J. Phys. Chem. B* **104** 8925 (2000)
59. A Henglein, M Giersig *J. Phys. Chem. B* **104** 5056 (2000)
60. A Henglein *J. Phys. Chem. B* **104** 6683 (2000)
61. J H Hodak, A Henglein, G V Hartland *J. Phys. Chem. B* **104** 9954 (2000)
62. J H Hodak, A Henglein, G V Hartland *Pure Appl. Chem.* **72** 189 (2000)
63. L D'Souza, S Sampath *Langmuir* **16** 8510 (2000)
64. Y Mizukoshi, T Fujimoto, Y Nagata, R Oshima, Y Maeda *J. Phys. Chem. B* **104** 6028 (2000)
65. J L Rousset, F J C S Aires, B R Sekhar, P Melinon, B Prevel, M Pellarin *J. Phys. Chem. B* **104** 5430 (2000)
66. A A Novakova, O V Agladze, B P Tarasov *Zh. Neorg. Khim.* **45** 1288 (2000) [d]
67. A A Novakova, T Yu Kiseleva, V V Levina *Zh. Neorg. Khim.* **45** 1388 (2000) [d]
68. G B Sergeev, T I Shabatina, V N Soloviev, A V Nemukhin *Spectrochim. Acta, Part A* **56** 2527 (2000)
69. G B Sergeev, T I Shabatina, V N Soloviev, V V Zagorskii *Mol. Cryst. Liq. Cryst.* **356** 111 (2001)
70. T I Shabatina, A V Vlasov, E V Vovk, D J Stufkens, G B Sergeev *Spectrochim. Acta, Part A* **56** 2539 (2000)
71. G L Estiu, M G Gory, M Z Zerner *J. Phys. Chem. A* **104** 233 (2000)
72. E Apra, A Fortunelli *J. Mol. Struct. (Theochem)* **501 – 502** 251 (2000)
73. K M Neyman, N Rosch, G Pacchioni *Appl. Catal. A: General* **191** 3 (2000)
74. A Fortunelli, A M Velasco *J. Mol. Struct. (Theochem)* **528** 1 (2000)
75. E V Polikarpov, T I Shabatina, G B Sergeev, A V Nemukhin *Vestn. Mosk. Univ., Ser. 2, Khim.* **41** 283 (2000) [b]
76. T I Shabatina, E V Vovk, Yu N Morozov, V A Timoshenko, G B Sergeev *Mol. Cryst. Liq. Cryst.* **356** 143 (2001)
77. B M Sergeev, G B Sergeev, V A Kasaikin, E A Litmanovich, A N Prusov *Mol. Cryst. Liq. Cryst.* **356** 121 (2001)
78. B M Sergeev, V A Kasaikin, E A Litmanovich, G B Sergeev, A N Prusov *Khim. Fiz.* **19** 121 (2000) [e]
79. V E Bochenkov, N Stefan, L Brehmer, V V Zagorskii, G B Sergeev *Colloids Surf. A* (2001) (in the press)
80. V E Bochenkov, V V Zagorskii, G B Sergeev *Vestn. Mosk. Univ., Ser. 2, Khim.* **41** 327 (2000) [b]
81. V E Bochenkov, V V Zagorskii, G B Sergeev *Mol. Cryst. Liq. Cryst.* **356** 299 (2001)
82. T I Shabatina, A V Vlasov, G B Sergeev *Mol. Cryst. Liq. Cryst.* **356** 149 (2001)
83. S V Ivashko, V V Zagorskii, G B Sergeev *Mol. Cryst. Liq. Cryst.* **356** 443 (2001)
84. J-M Lehn *Supramolecular Chemistry. Concepts and Perspectives* (Weinheim: VCH, 1995)
85. C N R Rao, G U Kulkarni, P J Thomas, P P Edwards *Chem. Soc. Rev.* **29** 27 (2000)
86. S Fullam, S N Rao, D Fitzmaurice *J. Phys. Chem. B* **104** 6164 (2000)
87. A Kumar, A B Mandale, M Sastry *Langmuir* **16** 6921 (2000)
88. J Zheng, Z Zhu, H Chen, Z Liu *Langmuir* **16** 4409 (2000)
89. E Adachi *Langmuir* **16** 6460 (2000)
90. A K Boal, F Ilhan, J E DeRouchey, T Thurn-Albrecht, T P Russell, V M Rotello *Nature (London)* **404** 746 (2000)
91. B Nikoobakht, Z L Wang, M A El-Sayed *J. Phys. Chem. B* **104** 8635 (2000)
92. Y Wang, J Ren, K Deng, L Gui, Y Tang *Chem. Mater.* **12** 1622 (2000)
93. S Link, Z L Wang, M A El-Sayed *J. Phys. Chem. B* **104** 7867 (2000)
94. S Link, C Burda, B Nikoobakht, M A El-Sayed *J. Phys. Chem. B* **104** 6152 (2000)
95. S Chen *J. Phys. Chem. B* **104** 663 (2000)
96. S Chen *J. Am. Chem. Soc.* **122** 7420 (2000)
97. L Maya, G Muralidharan, T G Thundat, E A Kenik *Langmuir* **16** 9151 (2000)
98. O D Velev, E W Kaler *Adv. Mater.* **12** 531 (2000)
99. P M Tessier, O D Velev, A T Kalambur, J F Rabolt, A M Lenhoff, E W Kaler *J. Am. Chem. Soc.* **122** 9554 (2000)
100. H Fukushima, S Seki, T Nishikawa, H Takiguchi, K Tamada, K Abe, R J Colorado, M Graupe, O E Shmakova, T R Lee *J. Phys. Chem. B* **104** 7417 (2000)
101. L Motte, E Lacaze, M Maillard, M P Pileni *Langmuir* **16** 3803 (2000)
102. J F Kang, J Zaccaro, A Ulman, A Myerson *Langmuir* **16** 3791 (2000)
103. G Kalyuzhny, A Vaskevich, G Ashkenasy, A Shanzer, I Rubinstein *J. Phys. Chem. B* **104** 8238 (2000)
104. P Andre, A Filankembo, I Lisiecki, C Petit, T Gulik-Krzywicki, B W Ninham, M-P Pileni *Adv. Mater.* **12** 119 (2000)
105. A Filankembo, M P-Pileni *J. Phys. Chem. B* **104** 5865 (2000)
106. S Chen, A C Templeton, R W Murray *Langmuir* **16** 3543 (2000)
107. C S Ah, H S Han, K Kim, D-J Jang *J. Phys. Chem. B* **104** 8153 (2000)
108. C S Ah, H S Han, K Kim, D-J Jang *Pure Appl. Chem.* **72** 91 (2000)
109. D H Jeong, J S Suh, M Moskovits *J. Phys. Chem. B* **104** 7462 (2000)
110. D H Jeong, N H Jang, J S Suh, M Moskovits *J. Phys. Chem. B* **104** 3594 (2000)
111. L Francois, M Mostafavi, J Belloni, J-F Delouis, J Delaire, P Feneyrou *J. Phys. Chem. B* **104** 6133 (2000)
112. J H Hodak, A Henglein, G V Hartland *J. Chem. Phys.* **112** 5942 (2000)
113. R Houdre, H Benisty, C Weisbuch *J. Lumin.* **85** 271 (2000)
114. Y Shen, D Jakubczyk, F Xu, J Swiatkiewicz, P N Prasad, B A Reinhardt *Appl. Phys. Lett.* **76** 1 (2000)
115. Y Shen, C S Friend, Y Jiang, D Jakubczyk, J Swiatkiewicz, P N Prasad *J. Phys. Chem. B* **104** 7577 (2000)
116. F T Quinlan, J Kuther, W Tremel, W Knoll, S Risbud, P Stroeve *Langmuir* **16** 4049 (2000)
117. T Hirai, T Watanabe, I Komasawa *J. Phys. Chem. B* **104** 8962 (2000)
118. B A Korgel, H C Monbouquette *Langmuir* **16** 3588 (2000)
119. R Kho, C L Torres-Martinez, R K Mehra *J. Colloid Interface Sci.* **227** 561 (2000)
120. E Hao, T Lian *Langmuir* **16** 7879 (2000)
121. X Duan, C M Lieber *J. Am. Chem. Soc.* **122** 188 (2000)
122. X Duan, C M Lieber *Adv. Mater.* **12** 298 (2000)

123. J D Holmes, K P Johnston, R C Doty, B A Korgel *Science* **287** 1471 (2000)
124. M S Gudiksen, C M Lieber *J. Am. Chem. Soc.* **122** 8801 (2000)
125. V N Soloviev, A Eichhoefer, D Fenske, U Banin *J. Am. Chem. Soc.* **122** 2673 (2000)
126. V N Soloviev, A Eichhoefer, D Fenske, U Banin *J. Am. Chem. Soc.* **123** 2354 (2001)
127. J Z Zhang *J. Phys. Chem. B* **104** 7239 (2000)
128. M Chen, Y Xie, H Chen, Z Qiao, Y Zhu, Y Qian *J. Colloid Interface Sci.* **229** 217 (2000)
129. D I Gittins, D Bethell, D J Schiffrin, R J Nichols *Nature (London)* **408** 67 (2000)
130. D I Gittins, D Bethell, R J Nichols, D J Schiffrin *J. Mater. Chem.* **10** 79 (2000)
131. D Feldheim *Nature (London)* **408** 45 (2000)
132. M Albrecht, M Lutz, A L Spek, G van Koten *Nature (London)* **406** 970 (2000)
133. J W Steed *Nature (London)* **406** 943 (2000)
134. R B Vasil'ev, A M Gas'kov, M N Rumyantseva, A S Ryzhikov, L E Ryabova, B Ya Akimov *Fiz. Tekh. Poluprovod.* **34** 993 (2000) [f]
135. B Sh Galyamov, S A Zav'yalov, L Yu Kupriyanov *Zh. Fiz. Khim.* **74** 459 (2000) [g]
136. A J Zarur, J Y Ying *Nature (London)* **403** 65 (2000)
137. J G McCarty *Nature (London)* **403** 35 (2000)
138. M Spiro, D M De Jesus *Langmuir* **16** 2464 (2000)
139. D M De Jesus, M Spiro *Langmuir* **16** 4896 (2000)
140. W Tu, H Liu, K Y Liew *J. Colloid Interface Sci.* **229** 453 (2000)
141. J Liu, Y Shin, Z Nie, J H Chang, L -Q Wang, G E Fryxell, W D Samuels, G J Exarhos *J. Phys. Chem. A* **104** 8328 (2000)
142. G Fagherazzi, P Canton, P Riello, F Pinna, N Pernicone *Catal. Lett.* **64** 119 (2000)
143. G Fagherazzi, P Canton, P Riello, N Pernicone, F Pinna, M Battagliarin *Langmuir* **16** 4539 (2000)
144. L Wang, M Rocci-Lane, P Brazis, C R Kannewurf, Y-I Kim, W Lee, J-H Choy, M G Kanatzidis *J. Am. Chem. Soc.* **122** 6629 (2000)
145. M M Maye, Y Lou, C-J Zhong *Langmuir* **16** 7520 (2000)
146. M M Maye, W Zheng, F L Leibowitz, N K Ly, C-J Zhong *Langmuir* **16** 490 (2000)
147. M M Maye, C-J Zhong *J. Mater. Chem.* **10** 1895 (2000)
148. C-W Chen, D Tano, M Akashi *J. Colloid Interface Sci.* **225** 349 (2000)
149. P Del Angel, J M Dominguez, G Del Angel, J A Montoya, E Lamy-Pitara, S Labruquere, J Barbier *Langmuir* **16** 7210 (2000)
150. M M Mohamed, T M Salama, M Ichikawa *J. Colloid Interface Sci.* **224** 366 (2000)
151. G Rupprechter, A S Eppler, A Avoyan, G A Somorjai *Stud. Surf. Sci. Catal. A* **130** 215 (2000)
152. A S Eppler, J Zhu, E A Anderson, G A Somorjai *Top. Catal. B* 33 (2000)
153. O V Zagorskaya, V Yu Zufman, T N Rostovshchikova, V V Smirnov, S P Gubin *Izv. Akad. Nauk, Ser. Khim.* 854 (2000) [a]
154. H Tada, K Teranishi, Y Inubushi, S Ito *Langmuir* **16** 3304 (2000)
155. J P Wilcoxon *J. Phys. Chem. B* **104** 7334 (2000)
156. C Blackledge, D A Engebreston, J D McDonald *Langmuir* **16** 8317 (2000)
157. S Hong, C Mirkin *Science* **288** 1808 (2000)
158. J J Storhoff, A A Lazarides, R C Mucic, C A Mirkin, R L Letsinger, G C Schatz *J. Am. Chem. Soc.* **122** 4640 (2000)
159. D-R Chen, C H Wendt, D Y H Pui *J. Nanopart. Res.* **2** 133 (2000)
160. C H Reynolds, N Annan, K Beshah, J H Huber, S H Shaber, R E Lenkinski, J A Wortman *J. Am. Chem. Soc.* **122** 8940 (2000)
161. S R Whaley, D S English, E L Hu, P F Barbara, A M Belcher *Nature (London)* **405** 665 (2000)
162. C A Mirkin, T A Taton *Nature (London)* **405** 626 (2000)
163. C A Mirkin *J. Nanopart. Res.* **2** 121 (2000)
164. P Ball *Nature (London)* **406** 118 (2000)
165. C Macilwain *Nature (London)* **405** 730 (2000)

[a] — *Russ. Chem. Bull. (Engl. Transl.)*
[b] — *Moscow Univ. Bull. (Engl. Transl.)*
[c] — *Polym. Sci. (Engl. Transl.)*
[d] — *Russ. J. Inorg. Chem. (Engl. Transl.)*
[e] — *Chem. Phys. Rep. (Engl. Transl.)*
[f] — *Semiconductors (Engl. Transl.)*
[g] — *Russ. J. Phys. Chem. (Engl. Transl.)*